Zootaxa 4286 (4): 451–482
http://www.mapress.com/j/zt/

Article

ISSN 1175-5326 (print edition)
ZOOTAXA
ISSN 1175-5334 (online edition)

https://doi.org/10.11646/zootaxa.4286.4.1
http://zoobank.org/urn:lsid:zoobank.org:pub:0005BE0C-51EB-4A89-83AD-B6B5CEA3A7B7

A morphological and molecular study of *Psilops*, a replacement name for the Brazilian microteiid lizard genus *Psilophthalmus* Rodrigues 1991 (Squamata, Gymnophthalmidae), with the description of two new species

MIGUEL TREFAUT RODRIGUES[1,10], RENATO RECODER[1], MAURO TEIXEIRA JR[1], JULIANA GUSSON ROSCITO[1], AGUSTÍN CAMACHO GUERRERO[1], PEDRO M. SALES NUNES[2], MARCO ANTONIO DE FREITAS[3], DANIEL SILVA FERNANDES[4], ADRIANA BOCCHIGLIERI[5], FRANCISCO DAL VECHIO[1], FELIPE SÁ FORTES LEITE[6], CRISTIANO DE CAMPOS NOGUEIRA[7], ROBERTA DAMASCENO[1], KÁTIA CRISTINA MACHADO PELLEGRINO[8], ANTÔNIO JORGE SUZART ARGÔLO[9] & RENATA CECILIA AMARO[1]

[1]*Universidade de São Paulo, Instituto de Biociências, Departamento de Zoologia, 05508-090, São Paulo, SP, Brazil*
[2]*Universidade Federal de Pernambuco, Centro de Biociências, Departamento de Zoologia, 50670-901, Recife, PE, Brazil*
[3]*Instituto Chico Mendes de Conservação da Biodiversidade, PARNA do Catimbau, 56537-000, Buíque, PE, Brazil*
[4]*Universidade Federal do Rio de Janeiro, Instituto de Biologia, Departamento de Zoologia. 21941-902, Rio de Janeiro, RJ, Brazil*
[5]*Universidade Federal de Sergipe, Centro de Ciências Biológicas e da Saúde, Departamento de Ecologia, 49100-000, São Cristóvão, SE, Brazil*
[6]*Universidade Federal de Viçosa, Campus Florestal, 35690-000, Florestal, MG, Brazil*
[7]*Universidade de São Paulo, Instituto de Biociências, Departamento de Ecologia Geral. 05508-090, São Paulo, SP, Brazil*
[8]*Universidade Federal de São Paulo, Departamento de Ciências Biológicas, 09972-270, Diadema, SP, Brasil*
[9]*Universidade Estadual de Santa Cruz, Programa de Pós-Graduação em Zoologia, 45662-900, Ilhéus, BA, Brazil*
[10]*Corresponding author. E-mail: mturodri@usp.br*

Abstract

The lizard genus *Psilophthalmus* was originally described from the sandy deposits at the northern end of Serra do Espinhaço, in Santo Inácio, state of Bahia, but since then it has been recorded in other Brazilian localities of the states of Bahia, Minas Gerais, and Sergipe. Here, we review the collected specimens based on molecular markers (mitochondrial 12S, 16S, ND4 and cyt *b*, and nuclear C-*mos* and NT3) and morphological evidence (external, hemipenial and osteological morphologies). In the course of our revision we find out that *Psilophthalmus* Rodrigues 1991 was preoccupied by *Psilophthalmus* Szépligeti 1902 (Hymenoptera, Braconidae). The replacement name *Psilops* is proposed for the genus for which we recognize three species, with *Psilops paeminosus* as type species. One of the new species is found along the high elevation areas of the Chapada Diamantina plateaus, state of Bahia, while the other occurs in the *cerrados* of "Serra Geral", in the occidental plateaus of that state. *Psilops paeminosus* comprises three distinct allopatric clades that, based on current evidence, cannot be diagnosed morphologically: one from the vicinities of the type locality, one from the lower São Francisco River, and a third from the uplands of Minas Gerais and southern inland Bahia. We keep the latter two as candidate species but defer their formal description until further evidence allows robust diagnosis. Derived clades of *Psilops* with shorter limbs have invaded hotter and drier environments, while mostly used sandy soils along their evolution.

Key word: Chapada Diamantina, Serra Geral, hemipenis, osteology, phylogeny, taxonomy

Introduction

The gymnophthalmid lizard genus *Psilophthalmus* Rodrigues 1991 was erected by monotypy to *Psilophthalmus paeminosus* Rodrigues 1991, based on specimens obtained at Santo Inácio, state of Bahia, Brazil (Rodrigues 1991b). At the time of its discovery, *P. paeminosus* was one among a large number of new squamates described and considered endemic from a sand dune area on the banks of the middle course of São Francisco River (Rodrigues

Accepted by S. Carranza: 2 May 2017; published: 4 Jul. 2017

1991a; Rodrigues & Juncá 2002). The type locality is situated on the first escarpments of Serra do Assuruá, which emerge from the sandy plains of the right bank of São Francisco River. Serra do Assuruá is one of northernmost extensions of the Serra do Espinhaço, a mountain chain extending from states of Minas Gerais to Bahia. Although there are sandy soils and some small dunes in Santo Inácio area, they are much less evident than those on the left side of the river that harbors the largest continental dune field of South America (Rodrigues 1996).

This sand dune system forms a distinctive, isolated, and geographically restricted habitat (around 7.000 km^2) in the core of Caatinga domain, an extensive semiarid region covering about 800.000 km^2 in northeastern Brazil (Rodrigues 1996; Rocha & Rodrigues 2005). Subsequent studies in the Caatinga region and adjacent ecosystems confirmed that most of the purportedly endemic squamates of that area are indeed restricted to psamophilic habitats surrounding the São Francisco dune region (Rodrigues 2003). Meanwhile, additional specimens of the genus have been found to inhabit sandy soil regions far from Santo Inácio area, in the states of Bahia, Minas Gerais and Sergipe (Delfim *et al.* 2006; Recoder & Nogueira 2007; Freitas *et al.* 2012; Garda *et al.* 2013; Magalhães *et al.* 2015; Thomassen *et al.* 2016). We became recently acquainted that *Psilophthalmus* Rodrigues, 1991 was preoccupied by *Psilophthalmus* Szépligeti 1902 a genus of Braconid wasps (Hymenoptera). Although *Psilophthalmus* Szépligeti, 1902 is presently a synonym of *Wesmaelella* Spinola, 1853 (Papp 2014), the name is available according to the Code. Accordingly, we take this opportunity to propose *Psilops* **nom. nov.** from the greek *psilo* (naked) and ops (*eye*) as a replacement name for *Psilophthalmus* Rodrigues, 1991, keeping *Psilops paeminosus* as its type species.

Understanding the diversification of *Psilops* across a climatic gradient is interesting because the genus stands in a basal position regarding the evolution of snake-like forms within the Gymnopthalmini tribe. Grizante *et al.* (2012) identified that across species of that tribe, more elongated and limb reduced forms occupied more arid regions (i.e. hotter and with less rainfall), a pattern also recovered by the examination of morphological traits of the, lacertoid form *Vanzosaura* (Recoder *et al.* 2013). An intrageneric analysis of climatic niches in *Psilops* based on a phylogenetic hypothesis can further enlighten the climate driven evolution of snake-like forms in elongated gymnophthalmid lizards as previously suggested (Rodrigues 1991a; Rodrigues *et al.* 2009).

Detailed morphological and molecular analyses of the newly collected specimens support the recognition of new species of *Psilops*. Our molecular results distinguish five highly geographically structured monophyletic clades within *Psilops*. However, morphological data derived from pholidosis, coloration, osteology, and hemipenis does not unambiguously diagnoses all clades. Although admitting the genetic distinctiveness of these five clades, to avoid paraphyly, we choose to describe only two new species, which can be clearly diagnosed morphologically, until new evidence provides further information on this matter.

Material and methods

Field sampling. The fieldwork was done in eight localities in the state of Bahia (Miguel Calmon, Morro do Chapéu, Mucugê, Paulo Afonso [Estação Ecológica do Raso da Catarina], Santo Inácio, Senhor do Bonfim, Vitória da Conquista, and Jaborandi), and in two municipalities in the state of Minas Gerais (Grão Mogol and Formoso [Parque Nacional Grande Sertão Veredas]). Specimens were collected by active search in sandy soil areas or with pitfall traps consisting of four buckets, ranging from 20 to 60L, disposed in Y shape: the central one connected to the peripheral ones by a 4m long plastic drift fence. In each locality all the available habitats were sampled.

Specimens were fixed in 10% formalin, preserved in 70% ethanol, and housed at the herpetological collections of Laboratório de Herpetologia do Instituto de Biociências da Universidade de São Paulo, Museu de Zoologia da Universidade de São Paulo (MZUSP) and Museu Nacional, Universidade Federal do Rio de Janeiro (MNRJ).

Molecular phylogeny. Twenty-five individuals of *Psilops* were sampled for the molecular study. Representatives from all subfamilies of Gymnophthalmidae were included as outgroups, resulting in a matrix of 41 terminals (Table 1).

We extracted DNA from tissue samples (liver or muscle) preserved in 100% ethanol following the methods from Fetzner (1999). For the molecular analysis, we used partial sequences of four mitochondrial markers, ribosomal RNA 12S and 16S (Palumbi 1996), and the protein-coding NADH4 (ND4) (Arévalo *et al.* 1994) and cytochrome b (cyt *b*) (Bickham *et al.* 1995); and two nuclear protein-coding genes, oocyte maturation factor Mos (C-*mos*) (Godinho *et al.* 2005) and Neutrophin—3 (NT3) (Townsend *et al.* 2008). All genes fragments were amplified using standard PCR protocols, with annealing temperatures of 54°C for ND4, 12S, C-*mos* and NT3, and

52°C for 16S and cyt *b*. Direct purification of PCR products was performed with Exonuclease I and Shrimp Alkaline Phosphatase [*USB* Corporation (OH) or Thermo Fisher Scientific Inc. (MA), US]. Both strands of each region were directly sequenced using the BigDye Terminator 3.0 cycle Sequencing kit (Applied Biosystems) according to manufacturer's protocol. PCR products were sequenced at Instituto de Química da Universidade de São Paulo and Instituto de Ciências Biomédicas da Universidade de São Paulo. Resulting sequences were manually edited in CodonCode Aligner v. 5.0.2. (http://www.codoncode.com), and aligned using Clustal W program (Higgings *et al.* 1994), embedded in software, MEGA v. 5, with default settings (Tamura *et al.* 2011). The protein coding genes ND4, cyt *b*, C-*mos*, and NT3 were translated into amino acids to check for alignment quality. Sequences were deposited in GenBank under the accession numbers KY978075-KY978223 (Table 1). The best-fit model for each partition under the Akaike Information Criterion (AIC) was selected in MrModeltest v.2.2 (Nylander 2004): GTR + I + G (cyt-*b*, ND4 and 16S); GTR + G (12S and C-*mos*) and HKY + I (NT3).

We conducted a Bayesian inference (BI) on a concatenated alignment, implementing two independent runs of 20 million generations each, four chains, and tree sampling at each 1,000 generations with Mr.Bayes 3.1.2 (Ronquist & Huelsenbeck 2003) (available at Cyberinfrastructure for Phylogenetic Research, CIPRES). We checked effective sample sizes and average standard of split frequencies in each independent runs using Tracer v.1.5 (Drummond & Rambaut 2007). Trees prior to stationary were discarded as burnin (25%), with a 50% majority rule consensus tree obtained from the remaining data points. We considered posterior probability (pp) equal to or higher than 0.95 as evidence of significant support for clades (Huelsenbeck & Ronquist 2001). We assessed the maximum likelihood (ML) tree after 100 runs plus 1,000 replicates of bootstrap in RAxML 7.3.1 (Stamatakis 2006) implemented in CIPRES. Nodes with bootstrap proportions (BP) equal to or higher than 70% were considered as well-supported (Hillis & Bull 1993), with caveats. We edited the trees with FigTree 1.4.0. (http://tree.bio.ed.ac.uk/software/figtree/). Uncorrected Da distances among main clades were calculated in DNAsp 5.10.01 (Librado & Rozas 2009).

Morphometry and pholidosis. For comparison purposes, in addition to the recently collected material, we also analyzed preserved specimens deposited at the herpetological collections of MZUSP, MNRJ and MUFAL (Museu de História Natural da Universidade Federal de Alagoas) (Appendix I).

Scale counts were made under a stereomicroscope Zeiss STEMI SV6, and nomenclature follows Rodrigues (1991b) and Recoder *et al.* (2014). The following scale counts were taken: number of dorsal transversal rows, between posterior margin of hindlimbs and interparietal (DOR); number of ventral transversal rows, between the cloacal plate and median interbrachial (VEN); gular transversal rows, from posterior pair of mentals to median interbrachial (GUL); scales around midbody (SAM); lamellae under the fourth toe (LFT); and fourth finger (LFF); number of smooth subcaudal scales, from vent until becoming keeled in a longitudinal row (SCA); total number of femoral pores (POR). Sex was determined by the presence (males) and absence (females) of femoral pores or by direct observation of gonads through dissection.

We obtained ten morphometric measurements with a digital caliper (to the nearest 0.01 mm) following the description given in Recoder *et al.* (2013): snout-vent length (SVL), taken from the border of cloaca to the tip of snout; trunk length between limbs (TRL), from the anterior margin of hindlimb to the posterior margin of forelimb; head width (HW), measured at widest point; head length (HL), from the anterior margin of tympanic aperture to the tip of the snout; femur length (FL), from knee to margin of the outer scale of the cloacal plate; tibia length (TL), from knee to margin of sole; foot length (FTL), from margin of sole to tip of the longest toe excluding claw; humeral length (HUL), from axilla to elbow; forearm length (FAL), from elbow to tip of the longest finger excluding claw, and tail length (TAL), from cloaca to the end of the tail in specimens with complete tails.

Assumptions of normality and homoscedasticity were evaluated using Kolmogorov-Smirnov and Levene's test, respectively (Zar 2014). We checked the distribution of variables with boxplots (not shown), excluded outliers (*i.e.* individuals shorter than 26.0 mm SVL), and $\log_{10}$ transformed measurements prior to analysis.

A principal component analysis (PCA) was performed to explore patterns of morphological variation among specimens. Each clade used in the morphological comparisons included both specimens from which we had molecular information and geographically and morphologically similar specimens absent in the molecular analyses. We tested for significant differences among clades in scale counts, with Kruskal-Wallis Test, in body size (SVL), with analysis of variance (ANOVA), and in body shape, with multivariate analysis of variance (MANOVA). Differences in relative sizes were tested with analysis of covariance (ANCOVA) using SVL as covariate. Because of missing data, TAL was not included in multivariate analysis. We performed all the morphological analyses for each sex separately.

TABLE 1. Species and specimens of *Psilops* and outgroup taxa included in the molecular reconstructions, with information on localities and GenBank accession numbers. Vouchers and field number acronyms are as follow: MZUSP=Museu de Zoologia da Universidade de São Paulo; MNRJ=Museu Nacional/UFRJ; AAG =Adrian Garda, Universidade Federal do Rio Grande do Norte, Rio Grande do Norte; LG=Laboratório de Citogenética de Vertebrados, MTR= Miguel Trefaut Rodrigues (Universidade de São Paulo). Politic units of Brazil are: Bahia (BA); Goiás (GO); Minas Gerais (MG); Mato Grosso (MT); Pará (PA); Pernambuco (PE); Rondônia (RO); São Paulo (SP).

Species	Voucher	Locality	12S	16S	cyt *b*	ND4	C-*mos*	NT3
P. mucugensis **sp. nov.** (Clade E)	MZUSP 96918	Mucugê, BA	KY978079	KY978102	KY978152	KY978177	KY978127	KY978202
P. mucugensis **sp. nov.** (Clade E)	MZUSP 106188	Mucugê, BA	KY978083	KY978108	KY978158	KY978183	KY978133	KY978208
P. mucugensis **sp. nov.** (Clade E)	MZUSP 106206	Morro do Chapéu, BA	KY978092	KY978117	KY978167	KY978192	KY978142	KY978217
P. mucugensis **sp. nov.** (Clade E)	MZUSP 106208	Miguel Calmon, BA	KY978093	KY978118	KY978168	KY978193	KY978143	KY978218
P. mucugensis **sp. nov.** (Clade E)	MZUSP 106209	Miguel Calmon, BA	KY978094	KY978119	KY978169	KY978194	KY978144	KY978219
P. mucugensis **sp. nov.** (Clade E)	AAG 7080	Palmeiras, BA	KY978095	KY978120	KY978170	KY978195	KY978145	KY978220
P. mucugensis **sp. nov.** (Clade E)	AAG 7186	Palmeiras, BA	KY978096	KY978121	KY978171	KY978196	KY978146	KY978221
P. paeminosus (Clade C)	MZUSP 106181	Grão-Mogol, MG	KY978084	KY978109	KY978159	KY978184	KY978134	KY978209
P. paeminosus (Clade C)	MZUSP 106190	Grão-Mogol, MG	KY978085	KY978110	KY978160	KY978185	KY978135	KY978210
P. paeminosus (Clade C)	MZUSP 106203	Vitória da Conquista, BA	KY978089	KY978114	KY978164	KY978189	KY978139	KY978214
P. paeminosus (Clade C)	MZUSP 106204	Vitória da Conquista, BA	KY978090	KY978115	KY978165	KY978190	KY978140	KY978215
P. paeminosus (Clade C)	MZUSP 106205	Vitória da Conquista, BA	KY978091	KY978116	KY978166	KY978191	KY978141	KY978216
P. paeminosus (Clade D)	MTR 21258	Santa Brígida, BA	KY978088	KY978113	KY978163	KY978188	KY978138	KY978213
P. paeminosus (Clade D)	MZUSP 106200	Santa Brígida, BA	KY978086	KY978111	KY978161	KY978186	KY978136	KY978211
P. paeminosus (Clade D)	MZUSP 106199	Raso da Catarina, BA	KY978087	KY978112	KY978162	KY978187	KY978137	KY978212
P. paeminosus (Clade D)	MZUSP 106215	Senhor do Bonfim, BA	KY978097	KY978122	KY978172	KY978197	KY978147	KY978222
P. paeminosus (Clade D)	MZUSP 106216	Senhor do Bonfim, BA	KY978098	KY978123	KY978173	KY978198	KY978148	KY978223
P. paeminosus (typical)	MTR 926038	Lagoa de Itaparica, BA	KY978076	KY978099	KY978149	KY978174	KY978124	KY978199
P. paeminosus (typical)	MTR 926081	Lagoa de Itaparica, BA	KY978077	KY978100	KY978150	KY978175	KY978125	KY978200
P. paeminosus (typical)	MTR 3527	Gameleira de Assuruá, BA	-	KY978105	KY978155	KY978180	KY978130	KY978205
P. paeminosus (typical)	MTR 5058	Santo Inácio, BA	AF420702	AF420710	KT254380	AF420872	AF420825	KT254462
P. paeminosus (typical)	MTR 11142	Santo Inácio, BA	KY978082	KY978107	KY978157	KY978182	KY978132	KY978207
P. paeminosus (typical)	LG 1593	Santo Inácio, BA	KY978078	KY978101	KY978151	KY978176	KY978126	KY978201
P. seductus **sp. nov.** (Clade A)	MNJR 19102	Jaborandi, BA	-	KY978103	KY978153	KY978178	KY978128	KY978203
P. seductus **sp. nov.** (Clade A)	MNJR 19105	Jaborandi, BA	KY978080	KY978104	KY978154	KY978179	KY978129	KY978204

……*continued on the next page*

TABLE 1. (Continued)

Species	Voucher	Locality	12S	16S	cyt *b*	ND4	C-*mos*	NT3
Alopoglossus angulatus	MZUSP 89965 (LG 1026)	Guajará-Mirim, RO	AF420693	AF420744	KT254394	AF420909	AF420847	KT337452
Arthrosaura kockii	MTR 978011	Vila Rica, MT	AF420680	AF420721	KT254393	AF420866	KT254396	KT254464
Colobosaura modesta	MZUSP 89952 (LG 1145)	Niquelândia, GO	AF420666	AF420733	KT254367	AF420887	AF420845	KT337448
Calyptommatus nicterus	MTR 5053	Vacaria, BA	AF420684	AF420747	KT254372	AF420903	AF420822	KT254453
Caparaonia itaiquara	MZUSP 95061 (MTR 10848)	Caparaó, MG	KY978075	EU620438	KT254387	KT321358	KT254399	KT254446
Colobodactylus dalcyanus	MTR 936070 (LG 761)	Campos do Jordão, SP	AF420663	AF420736	KT254389	AF420881	AF420844	KT254445
Heterodactylus imbricatus	MTR 1524 (LG 1504)	Serra da Cantareira, SP	AF420661	AF420725	KT254388	AF420885	AF420835	KT254444
Iphisa elegans	MZUSP 82656 (MTR 977426)	Aripuanã, MT	AF420668	AF420714	KT254369	AF420889	AF420843	KT254447
Micrablepharus atticolus	MTR 946141	Santa Rita do Araguaia, GO	AF420664	AF420718	KT321348	AF420904	AF420826	KT254449
Micrablepharus maximiliani	MZUSP 89992 (LG 1017)	Barra do Garças, MT	AF420657	AF420730	KT254376	AF420875	AF420850	AF420875
Nothobachia ablephara	MTR 946245 (LG 897)	Petrolina, PE	AF420669	AF420740	KT254374	AF420900	AF420851	KT254457
Procellosaurinus erythrocercus	MTR 5057	Queimadas, BA	AF420679	AF420711	KT254377	AF420870	AF420836	KT254450
Procellosaurinus tetradactylus	MTR 5056	Alagoado, BA	AF420703	AF420713	KT254378	AF420871	AF420818	KT254451
Rhachisaurus brachylepis	MTR 887336	Serra do Cipó, MG	AF420665	AF420737	KT254392	AF420877	AF420853	KT254463
Tretioscincus oriximinensis	MTR 926415	Poção, PA	AF420691	AF420752	KT254385	AF420888	AF420846	KT337450
Vanzosaura multiscutata	MTR 5059	Vacaria, BA	AF420699	AF420716	KT254379	EU620442	AF420839	KT254452

Hemipenial morphology. We prepared the hemipenes of six individuals (MTR 11169, from Santo Inácio, Bahia; MZUSP 106186, from Gameleira do Assuruá, Bahia; 106196, from Miguel Calmon, Bahia; MNRJ 19099 and MNRJ 19103, from Jaborandi, Bahia; MTR 21617; from Vitória da Conquista, Bahia) representing four clades recovered in the *Psilops* phylogeny (see below), following the procedures described by Manzani and Abe (1988), modified by Pesantes (1994), and Zaher (1999). The retractor muscle was manually separated, and the everted organ filled with stained petroleum jelly. The organ was immersed in an alcoholic solution of red alizarin for 24 hours in order to stain eventual calcified structures (e.g., spines or spicules), in an adaptation proposed by Nunes *et al.* (2012) on the procedures described by Uzzell (1973) and Harvey and Embert (2008). The terminology of hemipenial structures follows previous literature (Dowling & Savage 1960; Savage 1997; Myers & Donnelly 2001; 2008; Nunes *et al.* 2012).

Osteology. We based the osteological description on four adult specimens (MZUSP 79584 and MZUSP 103258, from Santo Inácio, Bahia; MNRJ 19418, from Jaborandi, Bahia; and, MZUSP 96918, from Mucugê, Bahia). Specimens were double stained for cartilage and bone. The anatomical terminology follows Romer (1956), Russel and Bauer (2008), and Evans (2008).

Variation in niche envelope. We used all known localities from which *Psilops* have been recorded, including examined specimens (Appendix) and literature (Delfim *et al.* 2006) and extracted two sets of environmental variables: (1) climatic: the maximum temperature of the warmest month (BIO 5), the minimum temperature of the coldest month (BIO 6), and annual precipitation (BIO 12) (Hijmans *et al.* 2005), under 30s of resolution, as available in the WorldClim website (http://www.worldclim.org/), and; (2) soil: soil granulometry ranging from clay (class 1), through silt (class 6), to sand (class 12) (Batjes 2009), under 5 min resolution (http://www.webcitation.org/6l1cFx9Jt). We used these variables as they are easy to interpret and are known to have profound effect on Squamates physiology and morphology (Huey *et al.* 2009; Clusella-Trullas *et al.* 2011; Grizante *et al.* 2012; Recoder *et al.* 2013; Camacho *et al.* 2015). To compare environmental envelopes we plotted the variation in climatic and soil variables across clades, ordered based on their phylogenetic age, from oldest to more recent. In addition, we tested for differences in niche values among clades through a generalized least squares procedure in R, using the package nlme (Pinheiro *et al.* 2016).

Results

Molecular analysis. Our molecular analyses recovered five well supported (pp = 1; BP = 100%) main lineages within *Psilops* (Fig. 1): a lineage composed by individuals from Jaborandi, Bahia (Clade A), is sister to a lineage (pp = 1; BP = 100%) containing all remaining clades of *Psilops*; a second clade, formed by specimens from Lagoa de Itaparica, Santo Inácio and Gameleira do Assuruá, Bahia (Clade B), was recovered as sister to the clade comprising individuals from Grão Mogol, Minas Gerais, and Vitória da Conquista, Bahia (Clade C); this relationship was also well-supported (pp = 1; BP = 80%); both lineages C and D were retrieved as sisters to the clade including specimens from Senhor do Bonfim, Santa Brígida and Raso da Catarina, Bahia (Clade D); this relationship was also well-supported in the Bayesian analyses, but poorly supported in ML (pp = 1; BP = 54%); and individuals from Mucugê, Morro do Chapéu, Miguel Calmon and Palmeiras, Bahia, were retrieved as another well supported (pp = 1; BP = 97%) clade (Clade E).

Genetic divergence based on mitochondrial markers was high: among Clade A and remaining clades distances varied from 4 to 4.8 % for 16S; 7.2 to 8.1% for 12S; 9.6 to 13.3% for cyt *b*, and 12.8 to 13.4% for ND4 and among Clades B, C, D and E varied from 0.9 to 1.9% for 16S; 1.2 to 2.4% for 12S; 3.9 to 7.5% for cyt *b* and 3.8 to 7.8% for ND4 (Table 2). The divergence based on nuclear fragments was not so high as the mitochondrial markers, but still very significant: between Clade A and the others clades it was 3.1–4.6% for C-*mos* and 1.6-2.4% for NT3, and among Clades B, C, D and E it was 1.6–2.4% for C-*mos* and 0.8–1.1% for NT3.

Morphometry and pholidosis. We used data from 97 specimens in the morphological analyses: 11 from Clade A (eight males and three females), 17 from Clade B (12 males and five females), 21 from Clade C (11 males and ten females), 24 from Clade D (14 males and ten females), and 24 from Clade E (14 males and ten females). Scale counts were significantly different among clades (Kruskal–Wallis test, $p < 0.05$) except for VEN in females (Table 3). Clades C and E showed significantly higher numbers of DOR (both sexes) and VEN (males) compared to other groups. Clade E showed higher number of GUL compared to Clades B and D, despite overlap. Clade A

differed from the remaining clades by having significantly fewer LFT, LFF, POR and higher number of SAM. Clade A also showed fewer SCA than Clades C and E. Clade E differed from the remaining Clades by having higher number of SCA and POR. Clades B and D only differed in SAM (Table 3).

TABLE 2. Uncorrected Dna distances among 16S, cyt *b* and C-*mos* (below) and 12S, ND4 and NT3 (above) markers from the five main clades recovered in phylogenetic analyses.

16S/12S	A	B	C	D	E
A	-	0.074	0.081	0.074	0.072
B	0.040	-	0.013	0.013	0.019
C	0.048	0.019	-	0.012	0.021
D	0.044	0.011	0.019	-	0.024
E	0.047	0.012	0.017	0.009	-
Cyt *b*/ND4	A	B	C	D	E
A	-	0.132	0.128	0.133	0.134
B	0.133	-	0.058	0.049	0.052
C	0.122	0.069	-	0.078	0.057
D	0.096	0.060	0.075	-	0.038
E	0.105	0.039	0.074	0.041	-
C-*mos*/NT3	A	B	C	D	E
A	-	0.024	0.021	0.022	0.016
B	0.031	-	0.009	0.011	0.008
C	0.043	0.011	-	0.008	0.007
D	0.046	0.012	0.014	-	0.008
E	0.038	0.011	0.011	0.014	-

TABLE 3. Scale counts in the five clades of *Psilops* recovered in phylogenetic analyses. The average values, (minimum-maximum), and the results (*p*-value) of non-parametric Kruskal-Wallis tests for comparison among clades are presented. Number of individuals=N, Number of dorsals=DOR; number of ventrals=VEN; number of gulars=GUL; scales around midbody=SAM; lamellae under the fourth toe=LFT; lamellae under fourth finger=LFF; number of smooth scales under tail=SCA; and total number of femoral pores=POR.

	sex	N	DOR	VEN	GUL	SAM	LFT	LFF	SCA	POR
Clade A	F	3	38 (37–39)	26 (25–27)	8 (8–9)	22	15	9 (9–10)	3 (2–4)	-
	M	8	37 (36–38)	24 (22–25)	9 (8–10)	22	14 (13–16)	10 (9–11)	4	12 (10–12)
Clade B	F	5	37 (35–40)	26 (24–28)	8 (8–9)	20 (19–20)	17 (17–18)	12 (11–13)	3 (3–4)	-
	M	12	35 (34–36)	22 (21–24)	8 (7–9)	19 (19–20)	18 (16–20)	12 (11–13)	4 (3–6)	16 (15–16)
Clade C	F	10	39 (38–40)	26 (24–29)	9 (8–9)	19 (17–20)	18 (16–20)	12 (11–13)	6 (5–7)	-
	M	11	38 (37–39)	24 (23–26)	9 (8–10)	19 (17–20)	17 (15–19)	12 (11–13)	6 (5–7)	14 (14–15)
Clade D	F	10	38 (34–40)	25 (24–27)	8 (8–9)	19 (17–19)	17	12 (11–12)	5 (4–6)	-
	M	14	35 (34–37)	23 (21–24)	8	18 (17–19)	17	12 (11–13)	5 (4–5)	15 (13–16)
Clade E	F	10	37 (36–40)	26 (24–27)	9 (8–9)	18 (17–20)	17	12 (11–14)	10 (7–15)	-
	M	14	36 (34–38)	23 (22–24)	9 (8–10)	18 (17–20)	18	13 (11–14)	11 (7–14)	17 (16–20)
Kruskal-Wallis Test	F	38	< 0,05	0,224	< 0,05	< 0,01	< 0,05	< 0,05	< 0,01	-
	M	59	< 0,01	< 0,01	< 0,05	< 0,01	< 0,01	< 0,01	< 0,01	< 0,01

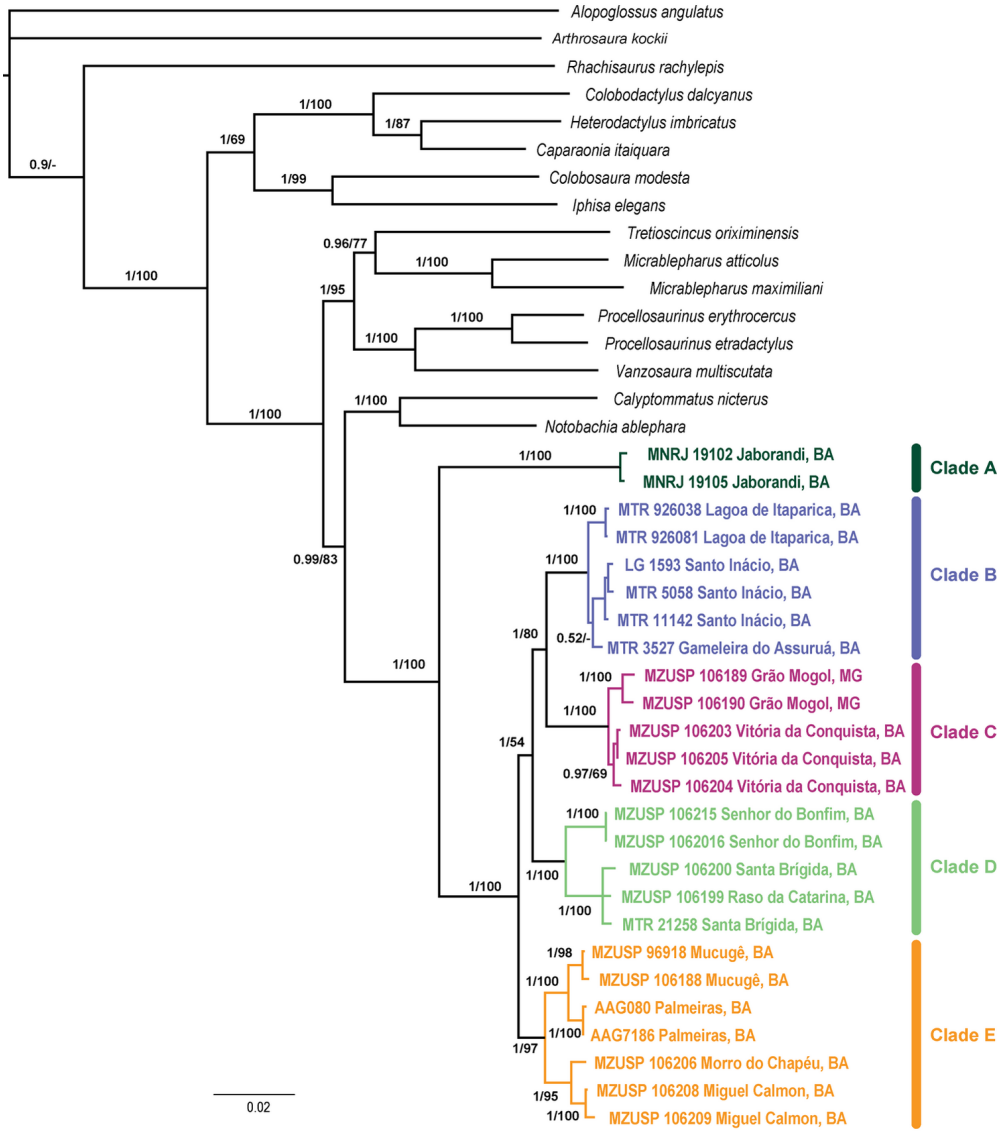

FIGURE 1. Phylogenetic inference of *Psilops* lineages based on combined analysis of mitochondrial (12S, 16S, ND4 and cyt *b*) and nuclear (C-*mos* and NT3) markers, under Bayesian analysis. Posterior probabilities (pp) and maximum likelihood bootstrap (BP) are depicted show above branches.

There was no significant difference in body size among clades of *Psilops* (ANOVA, $F_{1,20} = 2.11$, $p = 0.244$), but sexual dimorphism in size was significant ($F_{1,20} = 16.34$, $p < 0.01$), thus sexes were analyzed separately. Among clades, there were differences in body shape (males: Wilk's $\lambda = 0.01$, $F_{32,142} = 11.62$, $p < 0.01$; females: Wilk's $\lambda = 0.034$, $F_{16,32} = 8.80$, $p < 0.01$, as well as, in relative size for both males and females for all variables, $p < 0.01$) except TRL (Table 4). Thirty-four individuals had intact tails (36%); and the relative size of TAL did not differ among clades ($F_{4,34} = 0.255$, $p = 0.904$).

The first principal component based on meristic variables accounted for 49.5% of total variation in males, and 36.5%, in females, and they were negatively correlated with DOR, VEN and SAM and positively correlated with LFT, LFF SCA in both sexes; and, in males, the first principal component was also positively correlated with POR (Table 5). The second principal component explained 20.2% of the variation in males, and was highly and positively correlated with VEN and SCA. In females it explained 28.2% of the variation and was highly and positively correlated with DOR, VEN, and LFTL (Table 5). Considering the two principal components for both sexes, one can notice morphological differentiation among clades, except for clades B and D (Fig. 2).

The first principal component based on morphometric variables accounted for 76.3% of total variation in

males, and 72.6%, in females, and they were highly and positively correlated with all morphometric characters for both sexes (Table 6). The second principal component explained 9.4% of the variation in males, and was highly and positively correlated with SVL, TRL and FTL, and negatively correlated with HUM and FAL. In females, it explained 16.4% of the variation and was highly and positively correlated with SVL and TRL, and negatively with HUM and FAL (Table 6). The second principal component thus represents a contrast between body elongation and forelimb length. Most clades were distinguishable in the two principal components, for both sexes (Fig. 2). Interestingly, Clade B (type population) overlapped in morphospace with Clade D, but was distinct from its sister, Clade C.

TABLE 4. Morphometric measurements and comparisons among the five clades of *Psilops* recovered phylogenetically. The average values, minimum–maximum, and the results (*p*-value) of analysis of variance ANOVA (SVL) and ANCOVA (remaining variables) among clades are presented. Number of individuals=N; snout-vent length=SVL; trunk length between limbs=TRL; head width=HH; head length=HL; femur length=FEM; tibia length=TIB; foot length=FTL; humeral length=HUM; and forearm length=FAL.

	Sex	N	SVL	TRL	HW	HL	FEM
Clade A	F	2	33.1 (29.5–36.6)	19.8 (17.5–22.2)	3.9 (3.6–4.2)	5.8 (5.5–6.2)	3.4 (3.0–3.8)
	M	8	30.7 (26.5–32.8)	17.4 (15.8–18.6)	3.7 (3.3–4.0)	5.7 (5.1–6.2)	3.5 (3.1–3.9)
Clade B	F	3	32.2 (31.5–33.0)	19.8 (18.8–21.2)	3.4 (3.3–3.5)	5.2 (5.1–5.3)	2.9 (2.8–2.9)
	M	9	29.8 (26.9–33.5)	17.5 (15.6–20.1)	3.4 (3.0–3.9)	5.2 (4.8–5.4)	3.0 (2.5–3.4)
Clade C	F	10	33.5 (26.3–40.3)	20.6 (16.2–24.9)	3.5 (3.2–4.0)	5.5 (4.6–6.2)	3.1 (2.4–3.7)
	M	10	30.1 (26.3–33.5)	18.2 (15.3–20.0)	3.5 (3.0–3.9)	5.5 (4.9–6.0)	3.3 (2.7–4.1)
Clade D	F	8	34.8 (32.0–37.2)	21.9 (19.1–23.1)	3.5 (3.3–4.0)	5.3 (5.0–5.6)	3.3 (3.1–3.5)
	M	11	30.7 (26.0–33.1)	18.2 (15.6–19.3)	3.3 (2.7–3.7)	5.1 (4.7–5.4)	3.3 (2.9–3.5)
Clade E	F	8	34.0 (26.4–37.8)	20.7 (14.9–18.5)	3.8 (3.3–4.0)	5.7 (4.8–6.1)	3.6 (2.9–4.1)
	M	12	32.2 (28.2–35.4)	18.5 (16.2–20.2)	3,9 (3.5–4.3)	5.8 (5.1–6.7)	3.8 (3.3–4.2)
ANOVA/ ANCOVA	F	31	0.813	0.350	< 0.01	< 0.01	< 0.01
	M	50	0.129	0.014	< 0.01	< 0.01	< 0.01

continued.

	Sex	N	TIB	FTL	HUM	FAL
Clade A	F	2	2.8 (2.6–3.1)	4.6 (4.5–4.7)	2.3 (2.1–2.5)	4.5 (4.3–4.7)
	M	8	2.9 (2.5–3.1)	4.6 (4.3–5.0)	2.3 (2.0–2.6)	4.4 (4.0–4.9)
Clade B	F	3	2.6 (2.5–2.6)	4.8 (4.8–4.9)	1.9 (1.8–2.0)	3.6 (3.6–3.7)
	M	9	2.6 (2.4–2.9)	4.8 (4.5–5.2)	1.8 (1.5–2.0)	3.7 (3.5–4.1)
Clade C	F	10	2.8 (2.2–3.2)	5.2 (4.5–5.7)	2.1 (1.8–2.2)	4.3 (3.7–4.7)
	M	10	2.9 (2.3–3.2)	5.2 (4.3–5.7)	2,1 (1.8–2.5)	4.4 (4.0–4.8)
Clade D	F	8	2.7 (2.5–3.0)	5.1 (4.9–5.7)	1.8 (1.6–2.0)	3.9 (3.6–4.2)
	M	11	2.7 (2.4–3.0)	5.0 (4.7–5.4)	1.8 (1.7–2.1)	3.8 (3.5–4.1)
Clade E	F	8	3.1 (2.5–3.4)	5.6 (4.7–6.0)	2.3 (1,9–2.5)	4.8 (4.2–5.1)
	M	12	3.2 (2.7–3.6)	5.8 (5.1–6.3)	2.3 (2.0–2.7)	5.0 (4.6–5.4)
ANOVA/ ANCOVA	F	31	< 0.01	< 0.01	< 0.01	< 0.01
	M	50	< 0.01	< 0.01	< 0.01	< 0.01

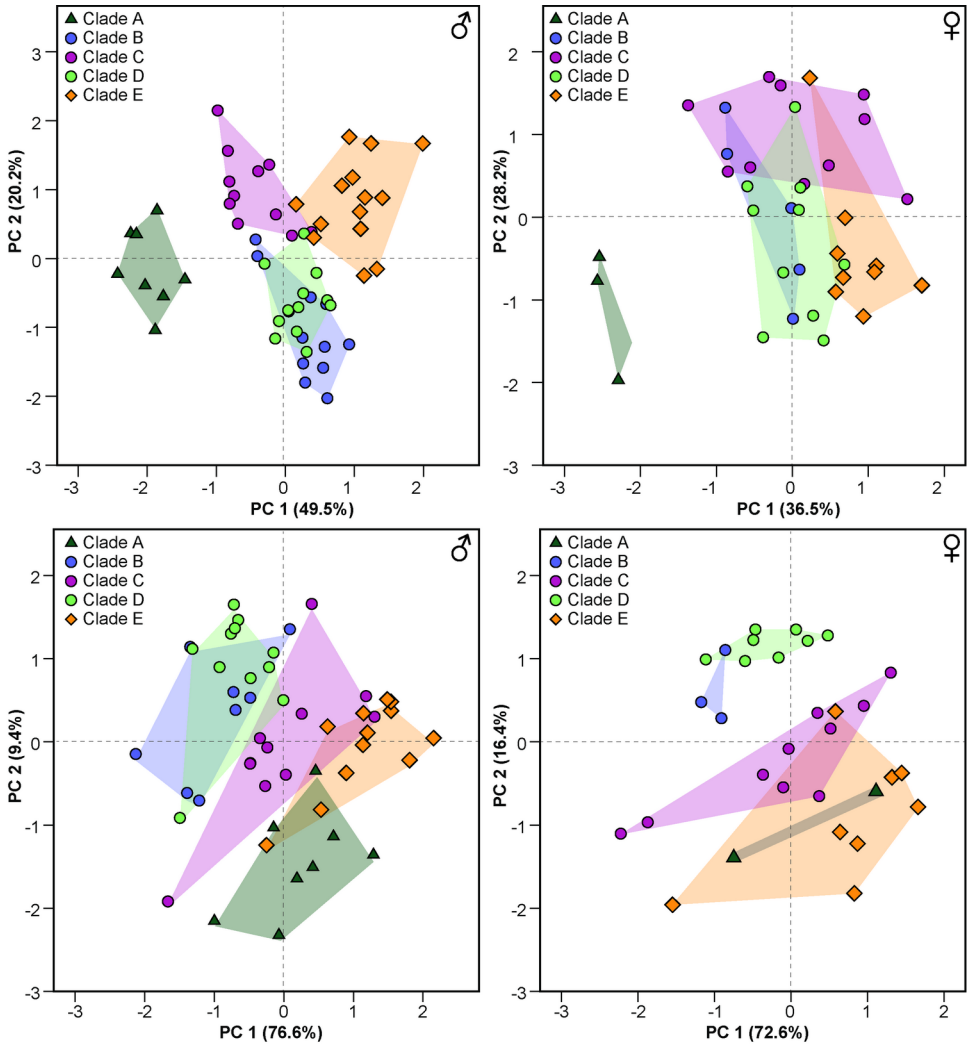

FIGURE 2. Ordination diagram of a principal component analysis upon meristic (top) and morphometric (bottom) data across *Psilops* clades.

TABLE 5. Results of principal component analysis (PCA) on seven meristic characters of *Psilops* clades. Number of dorsal scales=DOR; number of ventral=VEN; number of gulars=GUL; scales around midbody=SAM; lamellae under the fourth toe=LFT; lamellae under fourth finger=LFF; number of smooth scales under tail=SCA; and total number of femoral pores=POR.

	Males		Females	
Variables	PC1	PC2	PC1	PC2
DOR	-0.568	0.573	-0.283	0.807
VEN	-0.390	0.810	-0.534	0.677
SAM	-0.764	-0.099	-0.788	-0.053
LFT	0.768	0.017	0.532	0.647
LFF	0.809	0.043	0.717	0.383
SCA	0.592	0.627	0.640	-0.111
POR	0.903	0.163	-0.283	0.807
Eigenvalues	3.468	1.416	2.193	1.690
% of variation	49.5	20.2	36.5	28.2
Cumulative %	-	69.7	-	64.7

TABLE 6. Results of principal component analysis (PCA) on nine morphometric characters of *Psilops* clades. Snout-vent length=SVL; trunk length between limbs=TRL; head width=HW; head length=HL; femur length=FL; tibia length=TL; foot length=FTL; humeral length=HUL; and forearm length=FAL.

	Males		Females	
Variables	PC1	PC2	PC1	PC2
SVL	0.802	0.458	0.836	0.522
TRL	0.654	0.632	0.766	0.613
HW	0.867	-0.120	0.833	-0.108
HL	0.908	-0.047	0.933	-0.034
FEM	0.924	0.157	0.937	0.064
TIB	0.958	0.123	0.976	-0.055
FTL	0.740	0.398	0.828	-0.030
HUM	0.891	-0.377	0.773	-0.528
FAL	0.910	-0.241	0.813	-0.510
Eigenvalues	0.013	0.002	0.013	0.003
% of variation	76.6	9.6	72.6	16.4
Cumulative %	-	86.1	-	89.0

FIGURE 3. Live specimens of *Psilops paeminosus* (Clade B—type lineage), from Santo Inácio, Bahia (A), MZUSP 106215 (Clade D), from Senhor do Bonfim, Bahia (B) and, MZUSP 106189 (Clade C), from Grão Mogol, Minas Gerais (C).

Taxonomic decision. Our molecular data shows strong genetic structure, with five allopatric and well-supported clades. The most external clade (Clade A, from the western upland plateau of Serra Geral, in Bahia and Minas Gerais states) is highly divergent genetically, and can be easily distinguished from the other clades based on morphometry and pholidosis. Among the remaining four clades, the one occurring in the northern portion of the Serra do Espinhaço, locally known as Chapada Diamantina (Clade E, from Mucugê, Morro do Chapéu, and Miguel Calmon), can also be readily distinguished from the others on morphological basis, despite the similar genetic divergence among them. Specimens of *Psilops* from Santo Inácio and nearby areas (Clade B) are also

morphologically distinct from its sister clade, from Grão Mogol and Vitória da Conquista (Clade C). Nevertheless, Clade B cannot be unequivocally distinguished from populations at lower São Francisco River and adjacencies in northern Bahia and Sergipe (Clade D). Thus, the recognition of all morphologically diagnosable lineages as full species would render *P. paeminosus* paraphyletic (Clade B and D). Thus, in order to avoid paraphyly or describing species lacking morphological unambiguous diagnosis, we refrain from naming all these clades herein until more robust data become available and provide further morphologically diagnostic features.

Clade B includes the type lineage of *Psilops paeminosus*, the single species of *Psilops*, therefore this name should be attributed to all populations assembled within Clades B, C, and D (Fig. 3). Clades A and E can be promptly distinguished from the others, and are formally described in the following section.

Species account

Psilops mucugensis sp. nov.

(Figs. 4–5)

Psilophthalmus sp.—Cassimiro and Rodrigues (2009: 49); Freitas *et al.* (2012: 18, 20, 22); Magalhães *et al.* (2015: 247, 249, 258, 261)

Holotype. an adult male, MZUSP 106188, collected by M.A. Freitas and T.F. Santos Silva on October 5th 2005 (field number MTR 11787) from Fazenda Três Irmãos (12°53'06"S 41°31'41"W, 1075 m above sea level, hereafter asl), district of Guiné, municipality of Mucugê, Serra do Espinhaço (Chapada Diamantina), Bahia, Brazil.

Paratypes. MZUSP 96918, 106187 (field number MTR 11520–21), collected on 8th October 2005 in the same locality and collectors as for the holotype.

Referred specimens. AAG 6640, 6652, 6663, 6692, 6715–6716, 7026, 7040–7041, 7065, 7080, 7109, 7120, 7142, 7144, 7190, 7199, 7220, 7228, 7249 from Palmeiras (12°32'S, 41°29'W), Bahia, Brazil; collected by Adrian Garda *et al*. on 6th January to 6th February 2013. MZUSP 106196, 106208, 106209 (all from 11°22'24.17"S, 40°31'4.22"W, 1141 m asl), MZUSP 106197 (11°22'23.74"S, 40°31'4.12"W, 1141 m asl), MZUSP 106210 (11°21'32"S, 40°31'37"W), all from Parque Estadual das Sete Passagens, municipality of Miguel Calmon: Bahia: Brazil; collected by the authors between 29th May 2010 to 10th March 2011, field numbers MTR 19871, RPD 040, RPD 110, MTR 20012, RPD 260, respectively. MZUSP 106206, from Morro do Chapéu hill (11°35'34.45"S, 41°12'27.65"W, 1271 m asl), municipality of Morro do Chapéu, Bahia, Brazil; collected by the authors on 30th December 2011, field number MTR 22533.

Diagnosis. *Psilops mucugensis* differs from *P. paeminosus* (data in parenthesis) by having a higher number of smooth subcaudal scales, 7–14 (3–7), a higher number of total pores, 16–20 (14–16), two conspicuous dorsolateral white stripes running from supraciliaries to the tail (absent), a bright red tail (brownish in adults) and longer forelimbs, 25.9% SVL (21.5% SVL). *Psilops mucugensis* differs from *P. seductus* **sp. nov.** (described below, data in parenthesis) by having lower number of scale rows around midbody, 17–21 (22), a higher number of subdigital lamellae under Finger IV, 16–19 (13–16) and Toe IV, 11–14 (9–11), a higher number of smooth subcaudal scales, 7–14 (2–5), a higher number of total pores, 16–20 (10–13), a larger foot, 17.6% SVL (14.8% SVL), and by the presence of calcified spines (absent) and by lacking papillae ornamenting the hemipenial flounces (present).

Description of the holotype. Rostral broad, visible from above wider than high, contacting first supralabial, nasal and frontonasal. Frontonasal hexagonal, slightly wider than long, in broad contact with rostral, nasal, prefrontals, and frontal. Prefrontals hexagonal, as long as wide, contacting frontonasal, frontal, first supraocular, first supraciliary, loreal, and nasal; separate at midline by contact between frontonasal and frontal. Frontal hexagonal with posteriorly convergent lateral margins, approximately twice as long as broad, wider anteriorly; in broad contact with first supraocular, its suture with frontonasal as broad as that of interparietal. Frontoparietals absent. Interparietal hexagonal, posteriorly rounded, with strongly posteriorly convergent lateral margins, longer than wide, longer and wider than frontal and contacting frontal, first supraocular, parietals, and occipitals. Parietals irregularly hexagonal, as long as wide, and smaller and shorter than interparietal, contacting first and second supraoculars, temporals, occipitals, and interparietal. Two supraoculars, first the largest, longer than wide, occupying most of supraocular area, second very small, sub-squared, with the same approximate size of the

adjacent temporal. Three supraciliaries, first slightly larger than second, third the smallest; first supraciliary expanding on the lateral face of head and in contact with loreal and preocular; second supraciliary in the center of eye. Nasal large, subrectangular, longer than wide, with the nostril in the center, contacting first and second supralabials. Loreal narrow, as high as nasal, diagonally oriented and contacting second and third supralabials, frenocular, first supraciliary, prefrontal and nasal. Frenocular as large as loreal with its postero-ventral corner divided in a small scute and followed posteriorly by a series of small and narrow irregular preoculars and suboculars. Seven supralabials, fourth the largest, under the eye, fifth the highest, separated from parietal by two

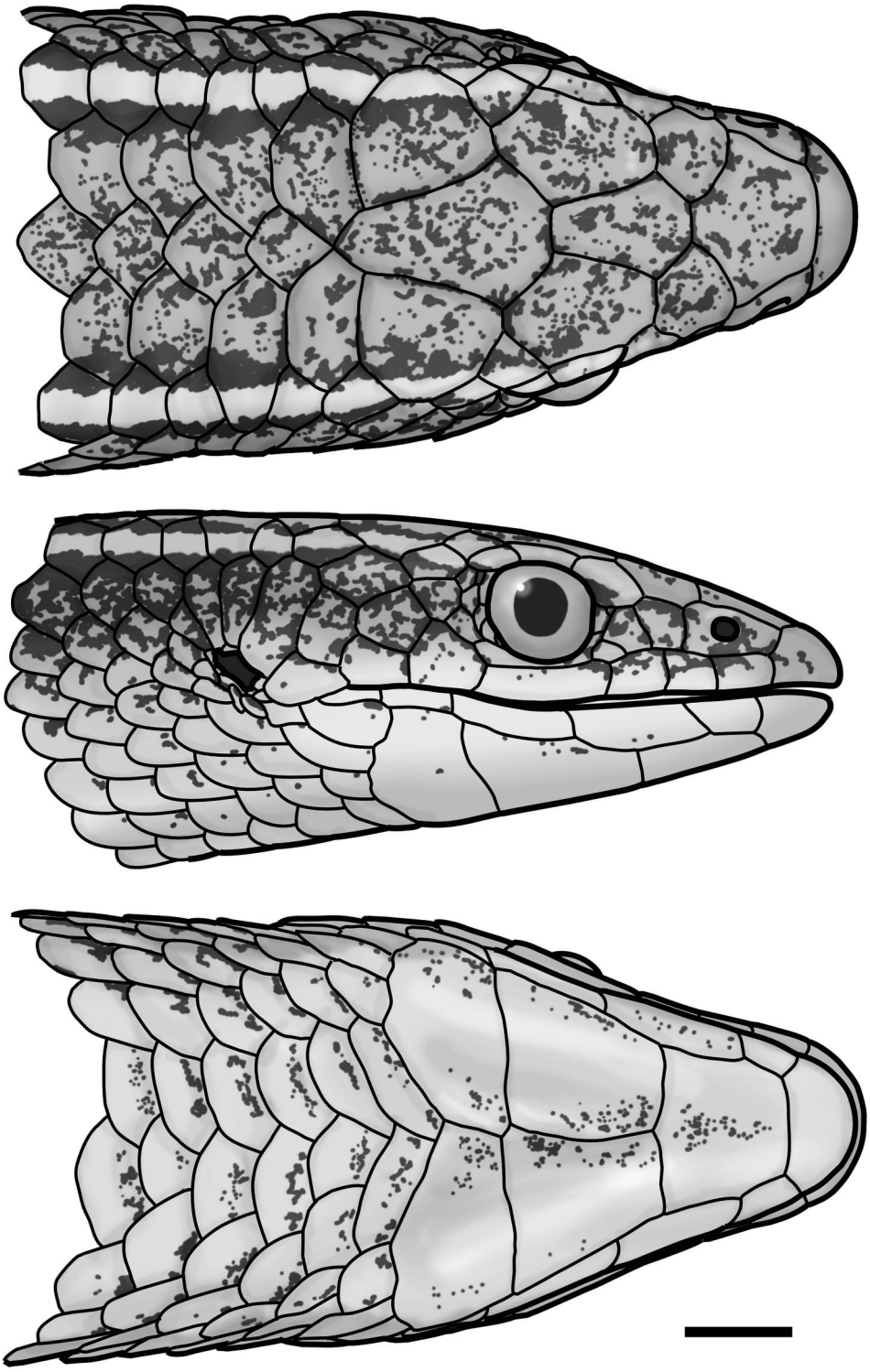

FIGURE 4. Dorsal (top), lateral (middle) and ventral (bottom) views of the head of the holotype of *Psilops mucugensis* (MZUSP 106188), from Mucugê, Bahia. Scale bar = 1 mm.

FIGURE 5. Live specimens of *Psilops mucugensis*, from Palmeiras (Photo by A. Garda) (A), MZUSP 106196, from Miguel Calmon (B) and MZUSP 106206, from Morro do Chapéu (C), Bahia.

postocular scutes; seventh supralabial contacting ear border. Eyelid absent. Eye large, pupil rounded. Anterior and lower margin of eye with an irregularly narrow, smooth, and elongate semidivided scute, thinner at lower margin of eye; posterior margin of eye with a series of juxtaposed smooth granules. Temporal region covered by enlarged, smooth, and imbricate cycloid scales. Tympanum recessed. Ear opening bordered by cycloid, smooth, and imbricate scales, those on posterior margin smaller, those above tympanum larger, higher than wide and covering anterior and superior margin of ear.

Mental wider than long. Postmental single, as wide as long, contacting first and second infralabials. Two pairs of enlarged genials in medial contact and contacting infralabials; first pair the largest, longer than wide, second one wider than long. Six infralabials, second and third the largest. All head scales smooth with irregularly disposed sensorial pits. Gulars disposed in nine irregularly transverse rows, smooth, imbricate, posteriorly rounded; central ones wider than long, diagonally disposed anteriorly, becoming gradually transverse posteriorly. Lateral gular scales smaller, cycloid, smooth, imbricate. Interbrachial row with five enlarged imbricate scales, central one the largest, subtriangular.

Anterior dorsal scales disposed in three longitudinal rows until the level of arm, dorsolateral ones wider than long, scales in central row smaller, as wide as long. Scales of the first transverse dorsal row smooth or slightly striate becoming gradually tri or pentacarinate. After arm level dorsal scales become progressively more elongate, mucronate and tricarinate, having the central keel sharper. Thirty-four transverse rows between interparietal and posterior level of hindlimbs. Lateral scales cycloid, smooth, imbricate, except for an area with small, flat, smooth and juxtaposed scales around arm insertion. Eighteen scales around midbody. Ventrals wide, smooth, imbricate, in four longitudinal rows from interbrachials to precloacals and in 24 transverse rows between interbrachials and precloacals. Central rows distinctively enlarged, wider than long. Posterior margin of vent with four scales; central ones smaller. Total pores 20, two precloacals and eight femoral on each side.

Scales of dorsal and lateral portion of tail imbricate, strongly keeled, elongate, mucronate, in complete rings; those covering dorsal portion of base of tail tricarinate, becoming unicarinate more elongate and lanceolate posteriorly. Scales of ventral portion of tail smooth, larger than correspondent dorsals at the base of tail but becoming gradually identical to them in shape and ornamentation toward the tip; 15 irregularly transverse rows of smooth subcaudals.

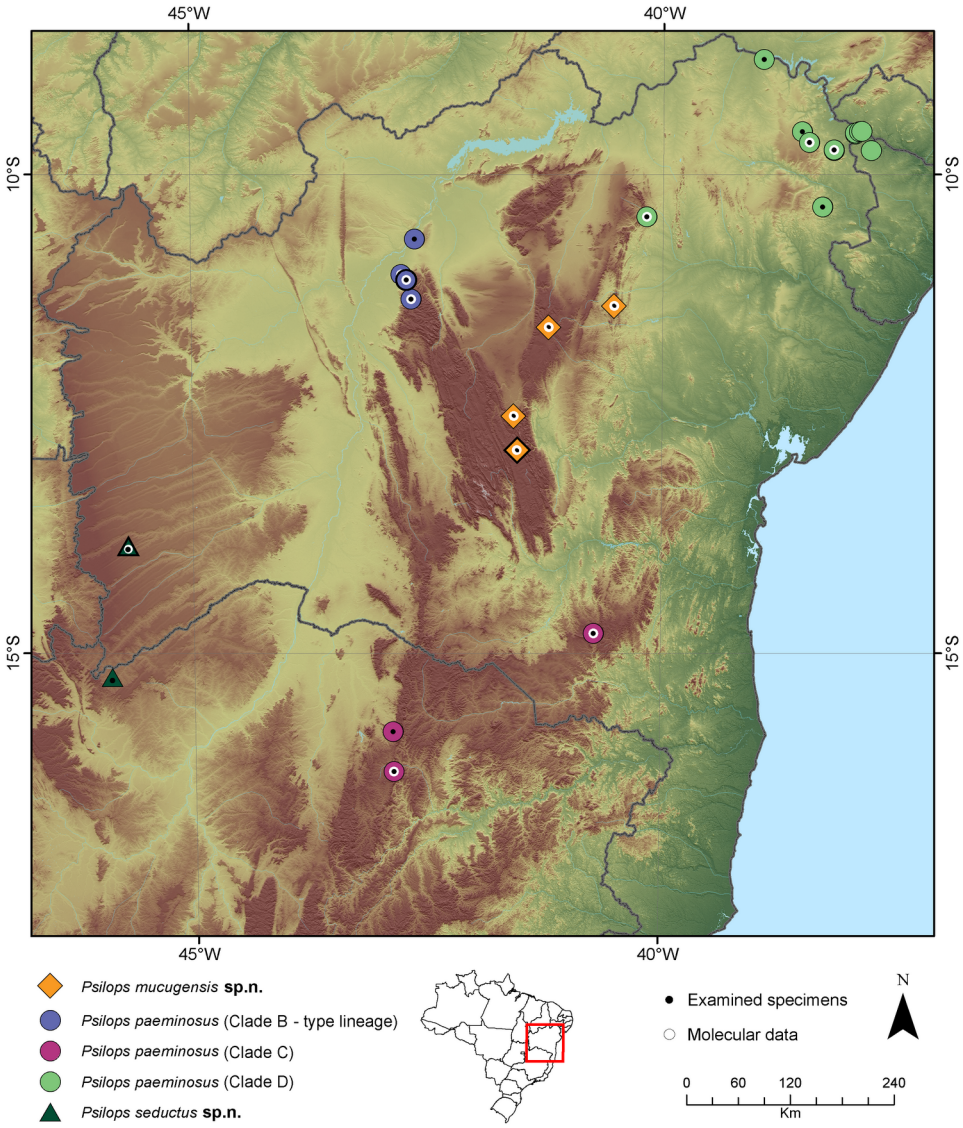

FIGURE 6. Map showing the known records of *Psilops*, including all clades of *P. paeminosus, P. seductus* and *P. mucugensis*; black central dots = localities from which specimens were examined; white central circle = localities from which molecular data were included in our analyses; symbols with bold outline = type localities.

Forelimbs with large, smooth and imbricate scales except for those on ventral parts of arm and forearm which are smaller. Anterior and posterior parts of tights with large, smooth and imbricate scales; posterior part of tights with granular, juxtaposed, smooth scales which grade progressively to a posterior irregular row of enlarged, mucronate, and keeled scales, identical to those covering dorsal part of tibia. Ventral parts of tibia with smooth, enlarged and imbricate scales. Palmar and plantar surfaces with small, conical, juxtaposed granules. Subdigital lamellae single, 12 on finger IV and 19 on toe IV. Fingers and toes clawed; first finger absent externally. Toes and fingers with the following relative sizes, respectively: 2=5<3<4 and 1<2<5<3<4.

Dorsal surface of body and tail olive brown with irregular and scattered dark brown reticulum. A dorsolateral white stripe runs from supraciliaries to the tail, becoming inconspicuous toward its extremity. Below it a dark brown lateral stripe extends from posterior margin of eye to tail. Between supraocular region and midbody the white stripe is also dorsally emarginated by an irregularly dark brown stripe which makes its anterior third highly conspicuous. Dorsal and lateral surfaces of head identical to corresponding parts of dorsum and flanks. Ventral parts of head, body, and tail creamy white with dark brown to black spots especially concentrated on external rows of ventral scales and in gular region which is mottled with dark spots. Limbs olive brown dorsally, mottled with darker pigment; ventrally creamy white, almost immaculate. Tail dorsal color identical to that of body proximally, becoming uniformly light brown posteriorly. Ventral portion of tail with dark spots proximally, creamily immaculate posteriorly.

Measurements. SVL= 35.3 mm; TAL = 42.3 mm (regenerated); TRL = 20.2 mm; HW = 4.3 mm; HL = 6.7 mm; FEM = 4.0 mm; TIB = 3.5 mm; FTL = 6.3 mm; HUM = 2.7 mm; FAL = 5.4 mm.

Variation. Individuals from southern (municipalities of Mucugê and Palmeiras) and northern (Morro do Chapéu and Miguel Calmon) populations, agree in most scale counts. Nevertheless, northern populations show fewer femoral pores (15–16, 16–20 in south) and number of smooth subcaudals (6–8, 10–14 in south) (Table 2). Males and females are sexually dimorphic in body size, with females having larger SVL than males (ANOVA; $F_{1,17}$ = 7,95; P < 0,05). Differences in shape are also significant, with females showing proportionally larger TRL (ANCOVA, SVL as covariate; $F_{1,16}$= 13.42; P < 0,01), but shorter HL ($F_{1,16}$= 13.67; P < 0,01), FEM ($F_{1,16}$= 12.37; P < 0.01) and TIB ($F_{1,16}$= 10.49; P < 0.01).

Distribution and natural history. Known from the municipalities of Mucugê, Palmeiras (Parque Nacional Chapada Diamantina), Morro do Chapéu and Miguel Calmon, state of Bahia, Brazil (Fig. 6). At Miguel Calmon it is found at high altitude open areas over quartzite sandy soils (1140 m asl), while at Morro do Chapéu, the single specimen was found within a semi-deciduous montane open forest (1270 m asl) (Fig. 7). At Mucugê it was found at a flat plateau (1100 m a.s.l.) covered by a type of low semi-deciduous arborescent vegetation. At Palmeiras it was found in areas of rocky grasslands *campos rupestres* (Magalhães *et al.* 2015).

Etymology. Named after the type locality, Mucugê, at Chapada Diamantina, Bahia.

FIGURE 7. Habitat occupied by *Psilops mucugensis* at Fazenda Três Irmãos, Mucugê (type locality) (A), and Morro do Chapéu (B), Bahia.

***Psilops seductus* sp. nov.**
(Figs. 8–9)

Psilophthalmus sp.—Nogueira (2006: 99–101, 128, 140, 192, 200–201, 227, 234, 237, 239, 244, 261, 294); Recoder and Nogueira (2007: 267, 270, 272–273, 278); Nogueira *et al.* (2009: 93); Nogueira *et al.* (2010: 356).

Holotype. an adult male MNRJ 19099, collected on 6th June 2008 by Adriana Bocchiglieri and Daniel Fernandes da Silva at Fazenda Jatobá (13°53' S, 45°42'W, 840 m a.s.l.), municipality of Jaborandi, Bahia, Brazil.

Paratypes. MNRJ 19097–98, MNRJ 19100–05, MNRJ 19417–18, same data as for the holotype, collected between January 2008 and December 2009.

Referred specimen. an adult male, MZUSP 94703 (field number CN 489), collected by Cristiano de C. Nogueira on 21st October 2001 at Grande Sertão Veredas National Park (15°15'13"S, 45°53'20"W, 795 m asl), municipality of Formoso, Minas Gerais, Brazil.

Diagnosis. *Psilops seductus* differs from *P. paeminosus* (data in parenthesis) by having a higher number of scale rows around midbody, 22 (17–20), a lower number of subdigital lamellae under Finger IV, 13–16 (15–20), and Toe IV, 9–11 (11–13), a lower number of total pores, 10–13 (14–16), and a red tail in adults (brown). It differs from *P. mucugensis* by having more scale rows around midbody, 22 (17–21), a lower number of subdigital lamellae under Finger IV, 13–16 (16-19) and Toe IV, 9–11 (11–14), a lower number of smooth subcaudal scales, 2–5 (7–14), a lower number of total pores, 10–13 (16–20), and a shorter foot, 14.8% SVL (17.6 %). Additionally, it differs from *P. paeminosus* and *P. mucugensis* in lacking calcified spines (present) and by having papillae ornamenting the hemipenial flounces (absent).

Description of the holotype. Rostral broad, visible from above wider than high, contacting first supralabial, nasal and frontonasal. Frontonasal hexagonal, slightly wider than long; in broad contact with rostral, nasal, prefrontals, and frontal. Prefrontals hexagonal, slightly longer than wide, contacting frontonasal, frontal, first supraocular, first superciliar, loreal, and nasal; separate at midline by contact between frontonasal and frontal. Frontal hexagonal with posteriorly convergent lateral margins, approximately one and half time as long as broad, wider anteriorly; in broad contact with first supraocular, suture with frontonasal much larger than that of interparietal. Frontoparietals absent. Interparietal hexagonal, posteriorly rounded, with strongly posteriorly convergent lateral margins, longer than wide, longer and wider than frontal and contacting frontal, first supraocular, parietals, and occipitals. Parietals irregularly hexagonal, as long as wide and smaller and shorter than interparietal, contacting first and second supraoculars, temporals, occipitals, and interparietal. Two supraoculars, first the largest, longer than wide, occupying most of supraocular area, second very small, subsquared, smaller than adjacent temporal. Three supraciliaries, second the largest, in the center of eye, third the smallest; first supraciliary expanded on lateral face of head and in contact with loreal and frenocular. Nasal large, subrectangular, longer than wide, with nostril in the center, contacting first and second supralabials. Loreal pentagonal, narrower than nasal, contacting second supralabial, frenocular, first supraciliary, prefrontal, and nasal. Frenocular contacting first supraciliary, a small preocular granule and an enlarged subocular which is thinner at the level of center of eye. Seven supralabials, fourth the largest, under the eye, fifth the highest, separated from parietal by two postocular scutes; seventh supralabial contacting ear border. Eyelid absent. Eye large, pupil rounded. Anterior margin of eye emarginated by first supraciliary, a preocular granule and a subocular, posterior margin of eye with a group of juxtaposed smooth granules and two postoculars. Temporal region covered by enlarged, smooth, and imbricate cycloid scales. Tympanum recessed. Ear opening bordered by cycloid, smooth, and imbricate scales, those on posterior margin smaller, those above tympanum larger than posterior ones and covering anterior and superior margin of ear.

Mental wider than long. Postmental single, slightly wider than long, contacting first and second infralabials. Two pairs of enlarged genials in medial contact and contacting infralabials, both wider than long, second the largest. Six infralabials, second and third the largest. All head scales smooth with irregularly disposed sensorial pits. Gulars disposed in 10 irregularly transverse rows, smooth, imbricate, posteriorly rounded; central and posterior ones wider than long, diagonally or transversally disposed. Lateral gular scales smaller, cycloid, smooth, imbricate. Interbrachial row with five enlarged imbricate scales, central one the largest and subtriangular.

First and second transverse rows of dorsal scales with three smooth and imbricate scales, external ones wider than long, modified as occipitals and post-occipitals and separated by a much smaller cycloid scale. Posterior to these differentiated rows dorsal scales are uni or tricarinate, transversely disposed, becoming progressively more

elongate, mucronate and tricarinate posteriorly. Thirty-six transverse rows of dorsals between interparietal and posterior level of hindlimbs. Lateral scales cycloid, smooth, imbricate, except for an area with small, flat, smooth and juxtaposed scales around arm insertion. Twenty-two scales around midbody. Ventrals wide, smooth, imbricate, in four longitudinal rows and twenty-three transversal rows in midline from interbrachials to precloacals. Central rows of ventral scales as wide as the external ones at midbody. Posterior margin of vent with four scales; central ones smaller. Total pores 12, two precloacals and four femorals on each side.

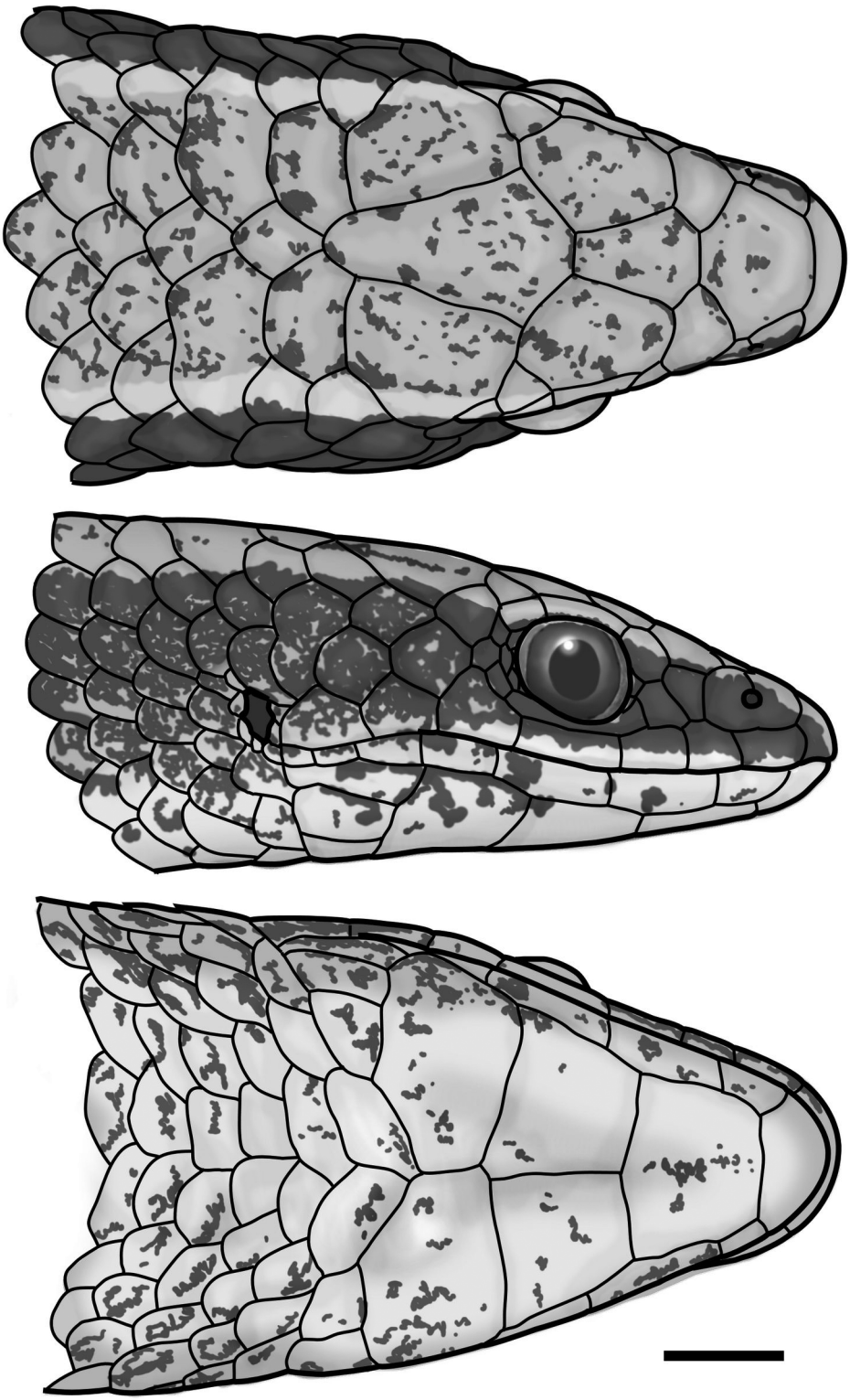

FIGURE 8. Dorsal (top), lateral (middle) and ventral (bottom) views of the head of the holotype of *Psilops seductus* (MNRJ 19099), from Jaborandi, Bahia. Scale bar = 1 mm.

FIGURE 9. Live specimens of *Psilops seductus*, MNRJ 19417, from Jaborandi, Bahia (A), and MZUSP 94703, from Formoso, Minas Gerais (B).

Scales of dorsal and lateral parts of tail imbricate, strongly keeled, uni or tricarinate, elongate, strongly mucronate, in complete rings, becoming more elongate and lanceolate posteriorly. Scales of base of tail smooth, larger than correspondent dorsals at the base of tail but becoming gradually identical to them in shape and ornamentation towards the tip.

Forelimbs with large, smooth, and imbricate scales except for those on ventral parts of arm and forearm which are smaller. Anterior and posterior parts of tights with large, smooth, and imbricate scales; posterior part of tights with granular, juxtaposed, smooth scales which grade progressively to a posterior irregular row of enlarged, mucronate, and keeled scales, identical to those covering dorsal part of tibia. Ventral parts of tibia with smooth, enlarged, and imbricate scales. Palmar and plantar surfaces with small, conical, juxtaposed granules. Subdigital lamellae single, nine on finger IV and 15 on toe IV. Fingers and toes clawed; first finger absent externally. Toes and fingers with the following relative sizes, respectively: 2=5<3<4 and 1<2<5<3<4.

Dorsal surface of body and tail iridescent olive brown with irregular and scattered dark brown reticulum. A dorsolateral thin and inconspicuous light white stripe runs from postocular region to the first third of body and becomes gradually inconspicuous posteriorly, merging with the dorsal color. Below it a wide dark brown lateral stripe reticulated with olive brown reaching the paraventral area, extends from posterior margin of eye to tail. Dorsal and lateral surfaces of head identical to corresponding parts of dorsum and flanks. Ventral parts of head, body, and tail creamy white with scattered slight dark brown to black spots that are especially concentrated in gular region. Limbs olive brown dorsally, mottled with darker pigment; ventrally creamy white, almost immaculate. Tail color identical to that of body proximally, becoming uniformly light brown posteriorly.

Measurements. SVL = 32.1 mm; TAL = 51.0 mm; TRL = 18.3 mm; HW = 3.9 mm; HL = 5.8 mm; FEM = 3.9 mm; TIB = 3.0 mm; FTL = 4.6 mm; HUM = 2.4 mm; FAL = 4.5 mm.

Variation. Little variation was observed in the type series. A single individual from the municipality of Formoso, Minas Gerais state (MZUSP 94703), agrees in all characters with type series, with scale counts falling within the variation observed (Table 2), except for a smaller number of femoral pores (10) than other males (12–13). Although the small sample of females precludes a quantitative analysis of sexual dimorphism, the largest female of *Psilops seductus* (36.6 mm SVL) was 1.12 times larger than the largest male (32.8 mm SVL).

Distribution and natural history. The only two localities from which it is known are located at "Serra dos Gerais" plateau (Fig. 6). The type locality, Fazenda Jatobá, is situated near the border between the states of Bahia, Minas Gerais and Goiás, an area dominated by extensive upland sandstone plateaus separated by river valleys, covered by different types of *cerrado* vegetation (Fig. 10). The Fazenda Jatobá is bounded by two rivers of the São Francisco basin (Arrojado and Veredãozinho) and has a total area of 92.000 ha, of which 40.000 ha were occupied by *Pinus* and *Eucalyptus* plantations. The remaining area is kept as a protected area with native *cerrado* (Fenger & Sevensson 2004). With an effort equivalent to 18.960 traps/day, 11 specimens were collected, seven in areas of continuous *cerrado*, three in areas of *Pinus* and *Eucalyptus* plantations, and one in a small fragmented *cerrado*. A single specimen (MZUSP 94703) was collected at a nearby locality, in Formoso, Minas Gerais, in Grande Sertão Veredas National Park, a large (230.714 ha) protected area at the border between Bahia and Minas Gerais. This specimen was collected in a pitfall trap within *carrasco* vegetation, a dense semideciduous arboreal phytophysiognomy occurring in isolated patches on top of the Serra Geral plateau, dominated by open *cerrado* savannas. Both *carrascos* and *cerrados* in Grande Sertão Veredas develop on flat, tabletop sandy soils (Recoder & Nogueira 2007). Besides a total of 180 lizards of 15 species captured in five sites in Grande Sertão Veredas NP, in a sampling effort of 3.400 trap x days, only a single specimen of the *Psilops seductus* was found (Nogueira *et al.* 2009).

FIGURE 10. Habitat occupied by *Psilops seductus* on *campo cerrado* (A), and *cerrado sensu stricto* (B), at Jaborandi, Bahia.

Etymology. from the Latin remote, apart, in reference to the geographic isolation of this species, which is restricted to the Cerrado plateaus of Serra Geral, west to the São Francisco River.

Hemipenial morphology

The following information is based on the hemipenes of three specimens of *Psilops paeminosus* (MTR 11169, MZUSP 106186, both in Clade B—type lineage, and MZUSP 106203, in Clade C), two specimens of *P. seductus* (MNRJ 19099 and MNRJ 19103) and one specimen of *P. mucugensis* (MZUSP 106196).

FIGURE 11. Hemipenes of *Psilops paeminosus* (MZUSP 106186, from Gameleira do Assuruá, Bahia) (Clade B—type lineage), in its sulcate, lateral and asulcate faces (A), *P. mucugensis* (MZUSP 106196, from Miguel Calmon, Bahia) (Clade E), in its sulcate and asulcate faces (B) and, *P. seductus* (MNRJ 19099, from Jaborandi, Bahia) (Clade A) (C). Scale bars = 1 mm.

The hemipenial morphology of the specimens of *Psilops mucugensis* and *P. paeminosus* (Clades B and C) are very conservative, revealing broadly similar organs. On the other hand, the morphology of the hemipenis of the two specimens of *P. seductus* revealed organs with considerably distinct morphology when compared to those of their congeners.

The hemipenes of all taxa are around 2 mm in total length, distinctly bilobed, with each lobe reaching approximately a fifth of the organ total length. Sulcus spermaticus broad and shallow running in a straight line through all hemipenial body to the region of lobular crotch, where it divides into two branches that run at the medial side of each lobe, ending among the folds that ornament the lobular apexes.

Hemipenial basis of *Psilops mucugensis* and *P. paeminous* distinctly narrower than the rest of hemipenis, providing a rough Y-shape. Hemipenial basis of *P. seductus* and the remaining hemipenial body broadly similar in width, providing a roughly cylindrical shape to the organ. Hemipenial body and lobes ornamented with 17–19 flounces encircling almost all the extension of the organ, crossing the full asulcate face and laterals and interrupting at the central sulcate face, at the two nude longitudinal columns that borders the *sulcus spermaticus*. Asulcate face with flounces diagonally directed towards lobes assuming a chevron-shape with vertex at the center of the face. *Psilops seductus* with five distalmost flounces curved at central asulcate face assuming a dome-shape with no vertex. *Psilops mucugensis* and *P. paeminosus* with flounces ornamented by two pairs of isolated, curved and calcified spines: one pair composed of one spine at each border of asulcate face and the other pair composed of one spine at each border of sulcate face. Sets of spines in each face border aligned in S-shape, particularly remarkable in those at the sulcate face borders. Specimens analyzed of *P. seductus* do not present any spine ornamentation on its flounces. On the other hand, the flounces of the hemipenis of *P. seductus* present distinct papillae, which are not visible in the hemipenis of the other taxa (Fig. 11).

Comparative Osteology

Both cranial and axial skeletons of the three species are quite similar, therefore the description below is representative of all species. The few, mainly quantitative differences, are stated along the description.

Cranial skeleton (Figs. 12–13): T-shaped premaxilla formed by alveolar plate with nine unicuspid pleurodont teeth and a narrow nasal process. Alveolar plate does not meet premaxillary process of maxilla. Nasal process separates nasals at midline and extends posteriorly to overlap frontal.

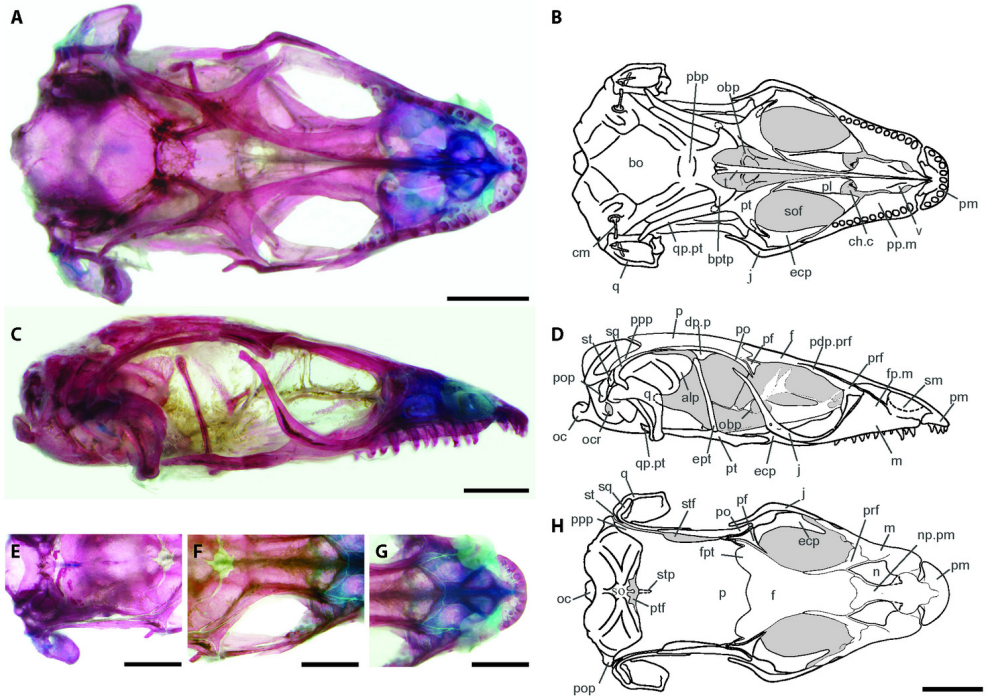

FIGURE 12. The skull of *Psilops seductus* (MNRJ 19418), in ventral (A–B) and lateral (C–D) views, middle, and anterior parts (E–G), and in dorsal view (H). Abbreviations: al, alar process; bo, basioccipital; bptp, basipterygoid process; ch.c, choanal channel; cm, columella; dp.p, descending process of the parietal; ecp, ectopterygoid; ept, epipterygoid; f, frontal; fp.m, facial process of the maxilla; fpt, frontoparietal tab; j, jugal; m, maxilla; n, nasal; np.pm, nasal process of the premaxilla; obp, orbitosphenoid; oc, occipital condyle; ocr, occipital recess; p, parietal; pbp, parabasisphenoid; pdp.prf, posterodorsal process of the prefrontal; pf, postfrontal; pl, palatine; pm, premaxilla; po, postorbital; pop, paroccipital process; pp.m, palatal plate of the maxilla; ppp, postparietal process; prf, prefrontal; pt, pterygoid; ptf, posttemporal fenestra; q, quadrate; qp.pt, quadrate process of the pterygoid; sm, septomaxilla; so, supraoccipital; sof, suborbital fenestra; sq, squamosal; st, supratemporal; stf, superior temporal fenestra; stp, sinotic tectum process; t, trabecula; v, vomer. Scale bars = 1mm.

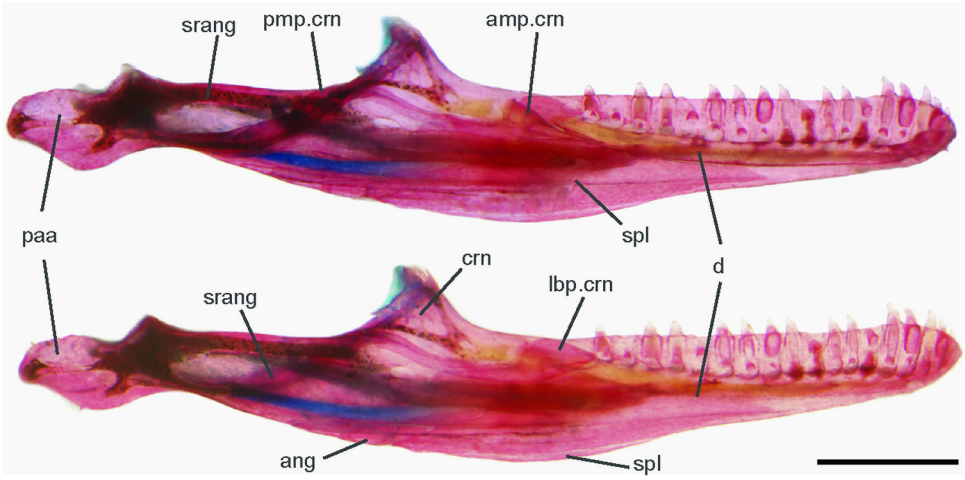

FIGURE 13. The mandible of *Psilops paeminosus* (MZUSP 79584) in lingual (top) and labial (bottom) views. Abbreviations: amp.crn, anteromedial process of the coronoid; ang, angular; crn, coronoid; d, dentary; lbp.crn, labial process of the coronoid; paa, prearticular-aricular complex; pmp.crn, posteromedial process of the coronoid; spl, splenial; srang, suprangular. Scale bar = 1mm

Maxilla extends anteriorly in an anteromedial process meeting palatal plate of premaxilla. Wide palatal shelf, bearing 11 teeth in *P. mucugensis*,12–13 in *P. paeminosus*, and 13 in *P. seductus*, extending posteriorly along vomer contacting maxillary process of palatine. Facial process of maxilla contacts nasal anteriorly, delimiting naris, overlapping anterior process of prefrontal posteriorly. Orbital process of maxilla contacts outer margin of ectopterygoid and supports maxillary process of jugal. Vomer with well-developed dorsal crest that holds, together with premaxilla and maxilla, the Jacobson's organ. Anterior process rests on a pit in palatal plate of premaxilla. Posteriorly, contacts ventral surface of palatine. Dome-shaped septomaxilla, located between vomer and nasal process of premaxilla, covers Jacobson's organ dorsally and laterally. Lateral maxillary process contacts dorsal surface of palatal shelf of maxilla. Nasal rests on dorsal surface of septomaxilla. Palatine with a wider anterior portion composed of medial vomerine process meeting vomer and lateral maxillary process contacting palatal shelf of maxilla; pronounced concavity between these processes forming choanal canal. Palatine ends posteriorly in a pterygoid process. Large prefrontal forms anterior margin of orbit, meeting facial process of maxilla and delimiting a lacrimal foramen. Lacrimal flange well-developed. Posterodorsal process of prefrontal forms part of dorsal margin of orbit, and its ventral process rests on dorsal surfaces of palatine and palatal shelf of maxilla, contacting maxillary process of jugal. Lacrimal absent. Anterior margin of frontal extends to level of septomaxilla, and bears a facet supporting posterior part of nasal. Anterolateral process absent. Posterior margin of frontal articulates with parietal by two fronto-parietal tabs overlapping corresponding surfaces of parietal. Posterolateral process well-developed, contacts postfrontal. Triangular postfrontal and elongated postorbital form part of posterodorsal margin of orbit. Postorbital meets temporal process of jugal anteriorly and squamosal posteriorly. Posterior end of squamosal fits into a notch on tympanic crest of quadrate. Parietal wide, forms skull roof along with frontal, meeting postfrontal and postorbital anterolaterally. Posteriorly, delimits with supraoccipital the post-temporal fenestra separated medially by ascending process of synoptic tectum, which fits into a pit on ventral surface of parietal. Post-parietal process long, extends posteriorly along transverse ridge of supraoccipital to meet squamosal and supra-temporal. Lateral descending process of the parietal short, approaches epipterygoid.

Thirteen bony sclerotic rings around the eye. Jugal delimits the lower and posterior margins of orbit, contacting maxilla and postorbital, bearing medially directed ectopterygoid process contacting ectopterygoid. Pterygoid large, Y-shaped; medial palatine process contacting palatine; lateral transverse process contacting posteromedial process of ectopterygoid. Medially, contacts basipterygoid process, bearing dorsally, a pit for rod-like epipterygoid. Quadrate process long, meeting mandibular condyle of quadrate. Three small pterygoid teeth present in *P. paeminosus*, two in *P. mucugensis*, absent in *P. seductus.* Cephalic condyle of quadrate meeting supratemporal and paroccipital process, lateral conch with a slight tympanic crest; mandibular condyle articulates with mandible. Suborbital fenestra is delimited by the vomer, maxilla, palatine, ectopterygoid and pterygoid. The upper temporal fenestra is delimited by the postfrontal, postorbital, squamosal, and parietal. Supraoccipital forms the roof of the

braincase and of the otic capsules, and the dorsal margin of the foramen magnum. It contacts laterally the prootic-otooccipital complex, which forms the lateral wall of the braincase. The alar process of the anterior margin of the prootic approaches the epipterygoid. The incisura prootica, below the alar process, forms a C-shaped exit for the trigeminal nerve. The facial foramen is located posteriorly to the incisura prootica. The crista prootica extends ventrally from this latter foramen to the parasphenoid. The vestibular and lagenar cavities are distinct in the internal surface of the prootic. Columella slender. Fenestra ovalis delimited anteriorly by prootic posteriorly by otooccipital. T-shaped extracolumella contacts internal surface of lateral conch of quadrate and paroccipital process. Horizontal and posterior semicircular canals seen dorsally to fenestra ovalis, and anterior semicircular canal extends into alar process.

Otooccipital, represented by fused opisthotic and exoccipital, contacts supraoccipital dorsally and basioccipital ventrally. Anterodorsal margin of opisthotic forming a well-developed paroccipital process. Occipital recess and vagus foramen delimited anteriorly by opisthotic and posteriorly by exoccipital, contributing to occipital condyle. Three foramina for hypoglossal nerve present. Ventral basioccipital contacts parabasisphenoid anteriorly and prootic and otooccipital laterally, forming most of occipital condyle. Parabasisphenoid fused to the basioccipital. Triangular orbitosphenoid connected to interorbital cartilages.

Mandible formed by dentary, splenial, angular, surangular, coronoid, and prearticular-articular complex. Dentary, bears 17–19 teeth; labial surface contacts splenial and small angular ventrally, surangular posteriorly, extending over labial process of coronoid; lingual surface with posterior margin of dentary overlapping splenial and anteromedial process of coronoid. Coronoid bears a large dorsal process, and a long posteromedial process, overlapping prearticular, forming anterior margin of adductor fossa. Splenial forms most of mid-lingual surface of mandible and shows alveolar and mylohyoid foramina. Surangular large, located posteriorly on labial surface of mandible, forming external margin of adductor fossa; surangular foramen large, a second smaller foramen also present. Prearticular-articular complex forms most of posterior end of lingual surface of mandible and floor and posterior margin of adductor fossa.

Hyoid apparatus composed of short basihyal, long glossohyal extending anteriorly, and three pairs of visceral arches: the hyoid cornu, directed anteriorly, bearing epihyal originating from its mid portions, extending posteriorly; first and second ceratobranchials, extending posteriorly.

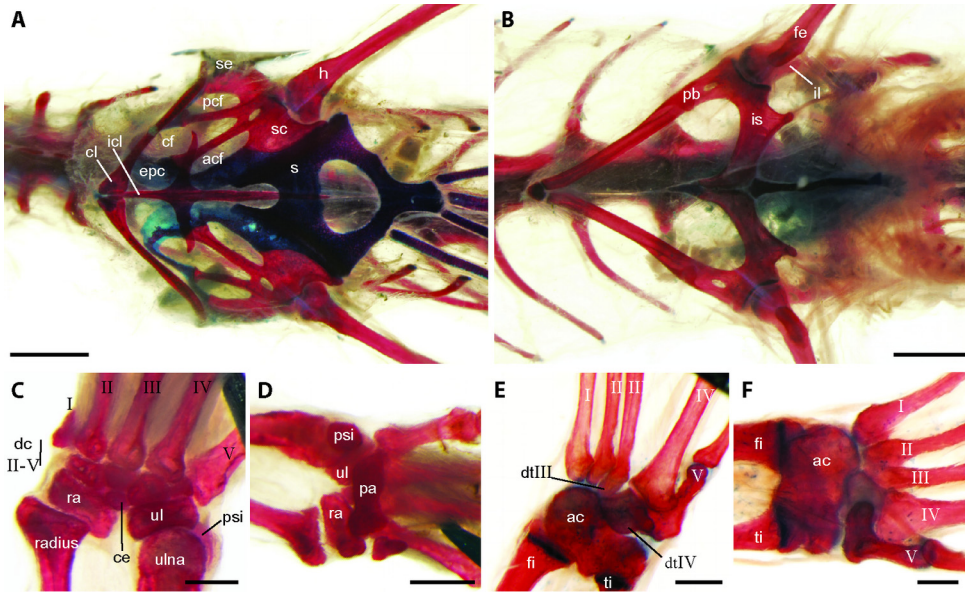

FIGURE 14. The appendicular skeleton of *Psilops paeminosus* (MZUSP 79584). Pectoral (A) and pelvic (B) girdles, in ventral view. Carpal region in ventral (C) and dorsal (D) views. Tarsal region in ventral (E) and dorsal (F) views, respectively. Abbreviations: ac, astragalus-calcaneus; acf, anterior coracoid foramen; ce, centrale; cf, coracoid foramen; cl, clavicle; dc, distal carpal; dt, distal tarsal; epc, epicoracoid; fe, femur; fi, fibula; h, humerus; icl, interclavicle; il, ileum; is, isquium; pa, palmar; pb, pubis; pcf, posterior coracoid foramen; psi, pisiform; ra, radiale; s, sternum; sc, scapulocoracoid; se, suprascapula; ti, tibia; ul, ulnare. Scale bars for A and B = 1mm; scale bars for C-F = 0.25mm.

Axial and appendicular skeletons: (Fig. 14) Axial and appendicular skeletons of all species of *Psilops* are also similar, and an in depth description of the axial and appendicular skeletons of *P. paeminosus*, which is representative of the other two species, can be found in Roscito and Rodrigues (2013). Still, minor differences can be seen between the species. The first difference concerns the number of presacral vertebrae: *P. paeminosus* and *P. mucugensis* have 30 vertebrae while *P. seductus* has 29 vertebrae. Another difference concerns the distal tarsal III (dtIII): while this element is clearly present in *P. seductus*, both *P. paeminosus* and *P. mucugensis* do not have a distinct dtIII, which is most likely fused to the 3rd metatarsal based on a slight suture between both elements seen in some specimens of *P. paeminosus*.

Niche evolution

Psilops clade diversified across a gradient of climatic conditions, with more recent lineages invading regions of higher thermal maxima and minima, and lower precipitation. Nonetheless, the group has remained restricted to silty-sandy soils across its evolution, as all specimens collected so far were found at soil granulometry ranging from silt to sand (Fig. 15, Table 7).

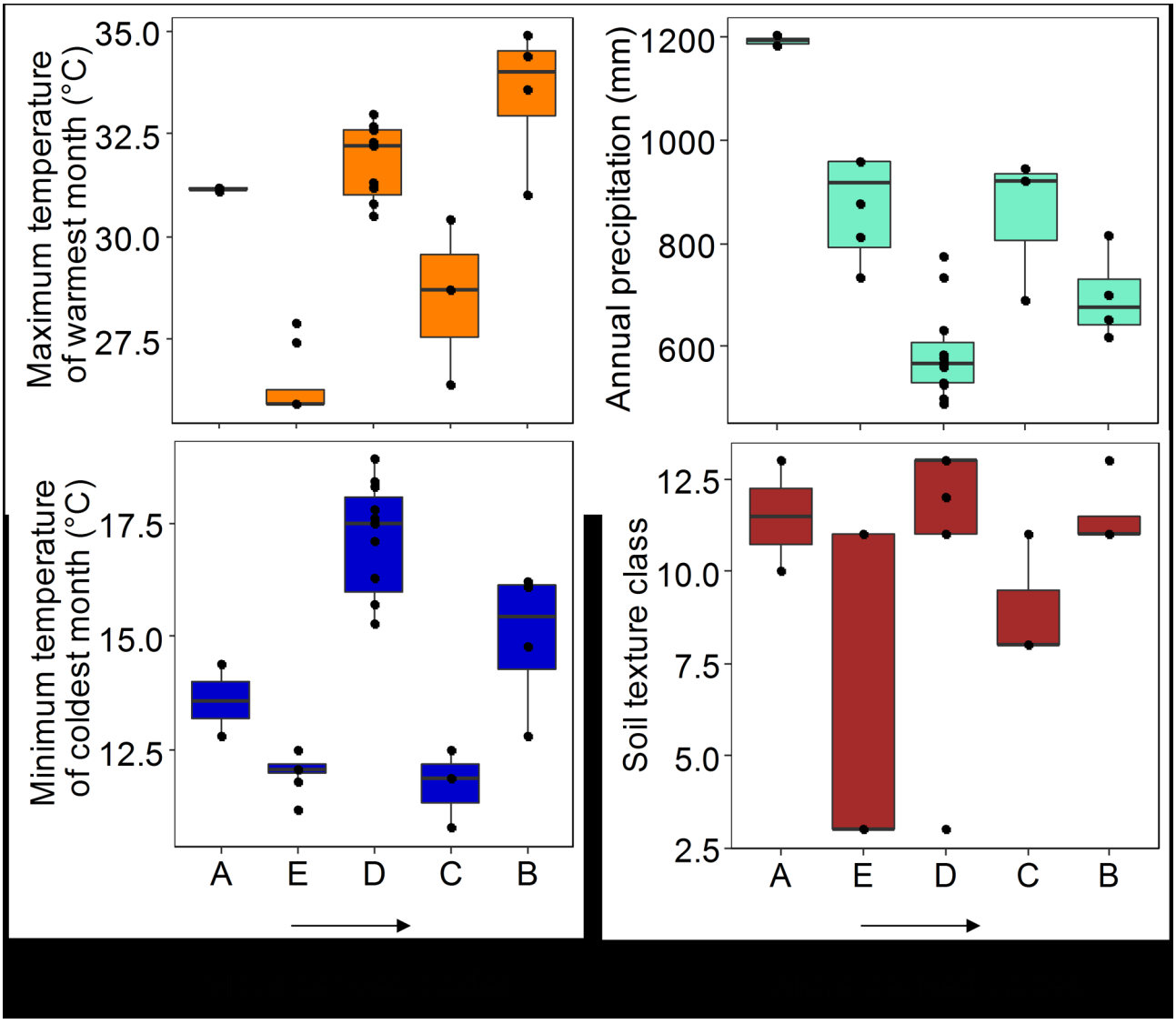

FIGURE 15. Niche envelope within the genus *Psilops*. Clades are ordered by their phylogenetic age, from oldest to most recent.

TABLE 7. Statistical variation in niche envelope traits across *Psilops* clades. While climatic envelope shows significant changes, soil type does not. Abbreviations: BIO 5=Maximum temperature of warmest month, BIO 6=Minimum temperature of coldest month, BIO 12=Annual precipitation, USDA soil class=Ranks for soil texture classes (see methods).

	BIO 5	BIO 6	BIO 12	USDA soil class
Clade A (intercept)	31.1 ± 0.8	13.6 ± 0.7	1193 ± 63.9	11.5±1.8
Clade B	1.9 ± 1.1	1.0 ± 1.0	-483.6 ± 90.4**	0.3±2.6
Clade C	-2.7 ± 1.19*	-1.9 ± 1.0	-363.4 ± 90.4**	-2.1±2.6
Clade D	0.6 ± 1.19	3.5 ± 1.0**	-577.3 ± 90.4**	-2.3±2.6
Clade E	-4.4 ± 1.2**	-1.7 ± 1.0	-337.6 ± 90.4**	-4.8±2.6

*p<0.05,**p<0.01

FIGURE 16. Habitat occupied by clades of *Psilops paeminosus*, at Santo Inácio (Clade B—type lineage) (A), Vitória da Conquista (Clade C) (B), and Senhor do Bonfim (Clade D) (C), Bahia.

Discussion

For centuries taxonomy has followed a morphological paradigm. Although its focus moved from a classical typological to the evolutionary and cladistics schools, morphological differences remained the groundwork to diagnose and infer historical relationships between taxa. The recent contributions of molecular approaches has allowed access to genetic information and thus to the history of lineages, independently from morphology. This turning point highlighted cryptic diversity in many groups where species formerly admitted as cohesive morphologically revealed to be highly structured genetically (Bickford *et al.* 2007; Albert & Fernandez 2009; Trontelj & Fišer 2009; Angulo & Icochea 2010; Cook *et al.* 2012; Nunes *et al.* 2012; Werneck *et al.* 2012; Anderson *et al.* 2013; Torres-Carvajal & Mafla-Endara 2013; Caminer & Ron 2014; Teixeira Jr *et al.* 2015; Acevedo *et al.* 2016; Arteaga *et al.* 2016). Nonetheless, as only in recent years we have been able to access this information in a more regular basis, we have not yet developed a theory on how to embed these data into the

taxonomic practice, which is still under a morphological paradigm, leading taxonomists to face a major challenge when describing species, as many of them remain undiagnosable morphologically.

This is the situation we face with some of the *Psilops* populations addressed in the present study. Molecular data indicated the existence of five allopatric, well-structured lineages, whereas only three of them are morphologically diagnosable from the typical lineage (Clade B). Although recognizing Clades B, C, and D, as candidate species and Clades B and C as morphologically diagnosable, we still cannot diagnose properly lineages B and D. Thereby, in order to avoid both paraphyly and describing a undiagnosable species, we prefer stay only with three names that can be unequivocally applied to those monophyletic lineages: *Psilops paeminosus* (Clades B, C and D), *P. mucugensis* (Clade E) and *P. seductus* (Clade A). It can be argued that this is an awkward decision. However, considering the relative rarity of these lizards, the fact that we still ignore the way the genetic clades approach geographically each other, and even that future misidentification based on geographic criteria could mask biological problems, our decision favors a less problematic and more practical taxonomy. We strongly believe that our choice will fuel molecular and morphological studies on the forthcoming collected specimens in order to have a better picture of their evolution.

Psilops paeminosus originally described from Santo Inácio, Bahia (Rodrigues 1991), is now a species composed by genetically divergent lineages, occurring at (1) Santo Inácio, Bahia, and its nearby areas, (2) the lower São Francisco River, in Bahia and Sergipe, and (3) the uplands of Planalto de Conquista, Bahia, and Espinhaço range, Minas Gerais (Fig. 6), usually associated with sandy soils from eroded quartzite outcrops (Fig. 16). *Psilops mucugensis* is restricted to Chapada Diamantina highlands and *P. seductus* to the flat sandstone plateaus of Serra Geral, western Bahia and Minas Gerais (Fig. 6). All species are in strict association with sandy soils. Recent biogeographical analyses (Nogueira *et al.* 2011; Azevedo *et al.* 2016) have recovered the isolated sandstone plateau of the Serra Geral as a biogeographical unit within the Brazilian Cerrado, harboring at least other four endemic squamates (Azevedo *et al.* 2016), roughly sympatric with *P. seductus*.

The most comprehensive molecular phylogeny of Teioidea places *Psilops* as sister to all other Gymnophthalmini (Goicoechea *et al.* 2016). Within the genus, the older divergence separate populations of western Cerrados in Bahia from a stock that remained historically associated to the Espinhaço range in the eastern bank of Rio São Francisco. It is interesting though that at the lower São Francisco River in Sergipe, *Psilops* stands restricted to the right bank of the river. This is an interesting contrast with other lizards like *Tropidurus semitaeniatus* (Werneck *et al.* 2015), for which there is no riverine barrier at that point.

Despite the old divergence from other genera and the strong genetic structure within *Psilops* its association with sandy habitats remained unaltered across time. This is reinforced by the fact that even though present species live in localities under contrasting climatic regimes, they do not show habitat shift. For instance, annual rain distribution and mean temperatures at Santo Inácio (600 m asl), near the lowlands close to São Francisco River, are strikingly different from those prevalent at the high elevations of Chapada Diamantina (above 1.000 m asl). These results are indicative that habitat preservation is crucial for maintenance and conservation of these evolutionary distinct lineages (Nimer 1972).

Squamate endemisms in cis-Andean South America has been previously reported for some lizards (Vanzolini & Ab'Saber 1968; Vanzolini & Gomes 1979; Rodrigues 1988), but were highlighted with the discovery of the sand adapted dune fauna of the middle Rio São Francisco (Rodrigues 1996). More recent examples of endemic species restricted to sandy soils were recently described in Central (Rodrigues *et al.* 2007; Teixeira Jr *et al.* 2013), and Northeastern Brazil (Rodrigues & Santos 2008). All these examples imply that we need to closely focus our conservation attention to those areas.

Body elongation and limb reduction in more recent lineages of *Psilops* match exposure to warmer and drier climates, which is in agreement with the patterns found by Grizante *et al.* (2012) and Recoder *et al.* (2013). Those results support the idea that elongation and limb reduction evolve as the lineage diversified to occupy habitats with more extreme temperatures (i.e. at least with higher upper extremes) (Rodrigues 1991a; Rodrigues *et al.* 2009). Functional analyses have recently shown that during such process, the development of burrowing behavior and occupation of sandy habitats is central for the evolution of such morphologies and their thermal physiology (Camacho *et al.* 2014). The results of our niche analysis support such view.

Acknowledgements

This work was funded by Fundação de Amparo à Pesquisa do Estado de São Paulo (FAPESP), Fundação de Amparo à Pesquisa do Estado do Rio de Janeiro (FAPERJ), and Conselho Nacional de Desenvolvimento Científico e Tecnológico (CNPq). We thank Floryl Florestadora Ypê S.A. and Jaborandi Agrícola Ltda for allowing the access to Jatobá Farm and Maria Júlia Martins Silva and André Faria Mendonça for providing logistical support, Maria Lucia Del Grande for the providing access and logistical support at Fazenda Esperança, at Vitória da Conquista, and Zélis Pereira and staff members for logistical support at Parque Estadual das Sete Passagens. José Mário Ghellere, Caroline Garcia, Milena Ferreira dos Santos, Eric Cazetta, Nayana Brito de Matos, Frederico França, Eduardo Varejão and Thaís Figueiredo Santos Silva helped in the field. We thank Sabrina Baroni, Maira Concistré, and Maysa Miceno for logistic support; Antonio Jorge Argolo (UESC), Hussam Zaher (MZUSP), Selma Torquato (MUFAL), Hugo Bonfim and Juliana Rodrigues Santos Silva (ICMBio) for the access to specimens under their care. Instituto Chico Mendes de Biodiversidade (ICMBIO) (permit numbers 11596, 14555 and 30309), Instituto Brasileiro do Meio Ambiente e dos Recursos Naturais Renováveis (IBAMA) (permit number 2001.007793/00-31) and Secretaria do Meio Ambiente do Estado da Bahia (permit number 13/2010), allowed the collection of specimens in the field.

References

Acevedo, A.A., Lampo, M. & Cipriani, R. (2016) The cane or marine toad, *Rhinella marina* (Anura, Bufonidae): two genetically and morphologically distinct species. *Zootaxa*, 4103 (6), 574–586.
https://doi.org/10.11646/zootaxa.4103.6.7

Albert, E.M. & Fernandez, A. (2009) Evidence of cryptic speciation in a fossorial reptile: description of a new species of *Blanus* (Squamata: Amphisbaenia: Blanidae) from the Iberian Peninsula. *Zootaxa*, 2234, 56–68.

Anderson, A.M., Stur, E. & Ekrem, T. (2013) Molecular and morphological methods reveal cryptic diversity and three new species of Nearctic Micropsectra (Diptera:Chironomidae). *Freshwater Science*, 32, 892–921.
https://doi.org/10.1899/12-026.1

Angulo, A. & Icochea, J. (2010) Cryptic species complexes, widespread species and conservation: lessons from Amazonian frogs of the *Leptodactylus marmoratus* group (Anura: Leptodactylidae). *Systematics and Biodiversity*, 8, 357–370.
https://doi.org/10.1080/14772000.2010.507264

Arévalo, E., Davis, S.K. & Sites, J.W. (1994) Mitochondrial DNA sequence divergence and phylogenetic relationships among eight chromosome races of the *Sceloporus grammicus* Complex (Phrynosomatidae) in Central Mexico. *Systematic Biology*, 43, 387–418.
https://doi.org/10.1093/sysbio/43.3.387

Arteaga, A., Pyron, R.A., Peñafiel, N., Romero-Barreto, P., Culebras, J., Bustamante, L., Yánez-Muñoz, M.H. & Guayasamin, J.M. (2016) Comparative phylogeography reveals cryptic diversity and repeated patterns of cladogenesis for amphibians and reptiles in Northwestern Ecuador. *PLoS ONE*, 11, e0151746.
https://doi.org/10.1371/journal.pone.0151746

Azevedo, J.A.R., Valdujo, P.H. & Nogueira, C.de C. (2016) Biogeography of anurans and squamates in the Cerrado hotspot: coincident endemism patterns in the richest and most impacted savanna on the globe. *Journal of Biogeography*, 43 (12), 2454–2464.
https://doi.org/10.1111/jbi.12803

Batjes, N.H. (2009) Harmonized soil profile data for applications at global and continental scales: updates to the WISE database. *Soil Use and Management*, 25, 124–127.
https://doi.org/10.1111/j.1475-2743.2009.00202.x

Bickford, D., Lohman, D.J., Sodhi, N.S., Ng, P.K.L., Meier, R., Winker, K., Ingram, K.K. & Das, I. (2007) Cryptic species as a window on diversity and conservation. *Trends in Ecology & Evolution*, 22, 148–155.
https://doi.org/10.1016/j.tree.2006.11.004

Bickham, J.W., Wood, C.C. & Patton, J.C. (1995) Biogeographic implications of cytochrome b sequences and allozymes in Sockeye (*Oncorhynchus nerka*). *Journal of Heredity*, 86, 140–144.
https://doi.org/10.1093/oxfordjournals.jhered.a111544

Camacho, A., Pavão, R., Moreira, C.N., Pinto, A.C.B.C.F., Navas, C.A. & Rodrigues, M.T. (2014) Interaction of morphology, thermal physiology and burrowing performance during the evolution of fossoriality in Gymnophthalmini lizards. *Functional Ecology*, 2015, 1–7.
https://doi.org/10.1111/1365-2435.12355

Caminer, M.A. & Ron, S.R. (2014) Systematics of treefrogs of the *Hypsiboas calcaratus* and *Hypsiboas fasciatus* species complex (Anura, Hylidae) with the description of four new species. *ZooKeys*, 370, 1–68.

https://doi.org/10.3897/zookeys.370.6291
Cassimiro, J. & Rodrigues, M.T. (2009) A new species of lizard genus *Gymnodactylus* Spix, 1825 (Squamata: Gekkota: Phyllodactylidae) from Serra do Sincorá, northeastern Brazil, and the status of *G. carvalhoi* Vanzolini, 2005. *Zootaxa*, 2008, 38–52.
Clusella-Trullas, S., Blackburn, T.M. & Chown, S.L. (2011) Climatic predictors of temperature performance curve parameters in ectotherms imply complex responses to climate change. *American naturalist*, 177, 738–751.
https://doi.org/10.1086/660021
Cook, G.M., Chao, N.L. & Beheregaray, L.B. (2012) Marine incursions, cryptic species and ecological diversification in Amazonia: the biogeographic history of the croaker genus *Plagioscion* (Sciaenidae). *Journal of Biogeography*, 2012, 724–738.
https://doi.org/10.1111/j.1365-2699.2011.02635.x
Delfim, F.R., Gonçalves, E.M. & Silva, S.T. (2006) Squamata, Gymnophthalmidae, *Psilophthalmus paeminosus*: distribution extension, new state record. *Check List*, 2, 89–92.
https://doi.org/10.15560/2.3.89
Dowling, H.G. & Savage, J.M. (1960) A guide to the snake hemipenis: a survey of basic structure and systematic characteristics. *Zoologica*, 45, 17–28.
Drummond, A.J. & Rambaut, A. (2007) BEAST: Bayesian evolutionary analysis by sampling trees. *BMC Evolutionary Biology*, 7, 1–8.
https://doi.org/10.1186/1471-2148-7-214
Evans, S.E. (2008) The skull of lizards and tuatara. *In:* Gans, C., Gaunt, A.S. & Adler, K. (Eds.), *Biology of the Reptilia. Vol. 20. Morphology H*. Society for the Study of Amphibians and Reptiles, Ithaca, pp. 1–347.
Fenger, C. & Sevensson, A. (2004) *The Environmental Factory Jatobá*. GAIA Publishing, Geneva, 128 pp.
Fetzner, J.W. (1999) Extracting high-quality DNA from shed reptile skins: a simplified method. *Biotechniques*, 26, 1052–1054.
Freitas, M.A., Veríssimo, D. & Uhlig, V. (2012) Squamate reptiles of the central Chapada Diamantina, with a focus on the municipality of Mucugê, state of Bahia, Brazil. *Check List*, 8, 16–22.
https://doi.org/10.15560/10.5.1020
Garda, A.A., Costa, T.B., Santos-Silva, C., Mesquita, D.O., Faria, R.G., Conceição, B.M., Silva, I.R.S., Ferreira, A.S., Rocha, S.M., Palmeira, C.N.S., Rodrigues, R., Ferrari, S.F. & Torquato, S. (2013) Herpetofauna of protected areas in the Caatinga I: Raso da Catarina Ecological Station (Bahia, Brazil). *Check List*, 9, 405–414.
https://doi.org/10.15560/9.2.405
Godinho, R., Crespo, E.G., Ferrand, N. & Harris, D.J. (2005) Phylogeny and evolution of the green lizards, *Lacerta* spp. (Squamata: Lacertidae) based on mitochondrial and nuclear DNA sequences. *Amphibia-Reptilia*, 26, 271–285. https://doi.org/10.1163/156853805774408667
Goicoechea, N., Frost, D.R., De la Riva, I., Pellegrino, K.C.M., Sites, J., Rodrigues, M.T. & Padial, J.M. (2016) Molecular systematics of teioid lizards (Teioidea/Gymnophthalmoidea: Squamata) based on the analysis of 48 loci under tree-alignment and similarity-alignment. *Cladistics*, 1–48.
https://doi.org/10.1111/cla.12150
Grizante, M.B., Brandt, R. & Kohlsdorf, T. (2012) Evolution of Body Elongation in Gymnophthalmid Lizards: relationships with Climate. *PLoS ONE*, 7, 1–7.
https://doi.org/10.1371/journal.pone.0049772
Harvey, M.B. & Embert, D. (2008) Review of Bolivian *Dipsas* (Serpentes: Colubridae), with comments on other South American species. *Herpetological Monographs*, 22, 54–105.
https://doi.org/10.1655/07-023.1
Higgins, D., Thompson, J., Gibson, T. Thompson, J.D., Higgins, D.G. & Gibson, T.J. (1994) CLUSTAL W: improving the sensitivity of progressive multiple sequence alignment through sequence weighting, position-specific gap penalties and weight matrix choice. *Nucleic Acids Res*, 22, 4673–4680.
Hijmans, R.J., Cameron, S.E., Parra, J.L., Jones, P.G. & Jarvis, A. (2005) Very high resolution interpolated climate surfaces for global land areas. *International Journal of Climatology*, 25, 1965–1978.
https://doi.org/10.1002/Joc.1276
Hillis, D.M. & Bull, J.J. (1993) An empirical test of bootstrapping as a method for assessing confidence in phylogenetic analysis. *Systematic Biology*, 42, 182–192.
https://doi.org/10.1093/sysbio/42.2.182
Huelsenbeck, J.P. & Ronquist, F. (2001) MRBAYES: Bayesian inference of phylogenetic trees. *Bioinformatics*, 17, 754–755.
https://doi.org/10.1093/bioinformatics/17.8.754
Huey, R.B., Deutsch, C.A., Tewksbury, J.J., Vitt, L.J., Hertz, P.E., Perez, H.J.A. & Garland, T. (2009) Why tropical forest lizards are vulnerable to climate warming. *Proceedings of the Royal Society B-Biological Sciences*, 276, 1939–1948.
https://doi.org/10.1098/rspb.2008.1957
Librado, P. & Rozas, J. (2009) DnaSP v5: a software for comprehensive analysis of DNA polymorphism data. *Bioinformatics*, 25, 1451–1452.
https://doi.org/10.1093/bioinformatics/btp187
Magalhães, F.M., Laranjeiras, D.O., Costa, T.B., Juncá, F.A., Mesquita, D.O., Röhr, D.L., Silva, W.P., Vieira, G.H.C. & Garda,

A.A. (2015) Herpetofauna of protected areas in the Caatinga IV: Chapada Diamantina National Park, Bahia, Brazil. *Herpetology Notes*, 8, 243–261.
Manzani, P.R. & Abe, A.S. (1988) Sobre dois novos métodos de preparo do hemipênis de serpentes. *Memorias do Instituto Butantan*, 50, 15–20.
Myers, C.W. & Donnelly, M.A. (2001) Herpetofauna of the Yutaje-Corocoro massif, Venezuela: Second report from The Robert G. Goelet American Museum–Terramar expedition to the northwestern tepuis. *Bulletin of the American Museum of Natural History*, 261, 1–85.
https://doi.org/10.1206/0003-0090(2001)261<0001:HOTYCM>2.0.CO;2
Myers, C.W. & Donnelly, M.A. (2008) The summit herpetofauna of Auyantepui, Venezuela: report from the Robert G. Goelet American Museum–Terramar Expedition. *Bulletin of the American Museum of Natural History*, 308, 1–147.
https://doi.org/10.1206/308.1
Nylander, J.A.A. (2004). MrModeltest v2. Evolutionary Biology Centre, Uppsala University. Available from: http://www.abc.se/~nylander/mrmodeltest2/mrmodeltest2.html (accessed 30 May 2017)
Nogueira, C. (2006) *Diversidade e Padrões de Distribuição da Fauna de Lagartos do Cerrado*. Ph.D. Thesis. Instituto de Biociências da Universidade de São Paulo, , São Paulo, 295 pp.
Nogueira, C., Colli, G.R., Costa, G.C. & Machado, R.B. (2010) Diversidade de répteis Squamata e evolução do conhecimento faunístico no Cerrado. *In:* Diniz, I.R., Marinho-Filho, J., Machado, R.B. & Cavalcanti, R.B. (Eds.), *Cerrado: Conhecimento Científico Quantitativo como Subsídio para Ações de Conservação*. Thesaurus, Brasília, pp. 329–372.
Nogueira, C., Colli, G.R. & Martins, M. (2009) Local richness and distribution of the lizard fauna in natural habitat mosaics of the Brazilian Cerrado. *Austral Ecology*, 34, 83–96.
https://doi.org/10.1111/j.1442-9993.2008.01887.x
Nogueira, C., Ribeiro, S., Costa, G.C. & Colli, G. (2011) Vicariance and endemism in a Neotropical savanna hotspot: distribution patterns of Cerrado squamate reptiles. *Journal of Biogeography*, 38, 1907–1922.
https://doi.org/10.1111/j.1365-2699.2011.02538.x
Nunes, P.M.S., Fouquet, A., Curcio, F.F., Kok, P.J.R. & Rodrigues, M.T. (2012) Cryptic species in *Iphisa elegans* Gray, 1851 (Squamata: Gymnophthalmidae) revealed by hemipenial morphology and molecular data. *Zoological Journal of the Linnean Society*, 166, 361–376.
https://doi.org/10.1111/j.1096-3642.2012.00846.x
Palumbi, S.R. (1996) Nucleic acids II: the polymerase chain reaction. *In:* Hillis, D.M., Moritz, C. & Mable, B.K. (Eds.), *Molecular Systematics*. Sinauer, Sunderland, MA, pp. 205–247.
Papp, J. (2014) A revisional study on Szépligeti's cardiochiline type specimens deposited in the Hungarian Natural History Museum, Budapest (Hymenoptera, Braconidae: Cardiochilinae). *Annales Historico-Naturales Musei Nationalis Hungarici*, 106, 169–214.
Pesantes, O.S. (1994) A Method for preparing the emipenis of preserved snakes. *Journal of Herpetology*, 28, 93–95.
https://doi.org/10.2307/1564686
Pinheiro, J., Bates, D., DebRoy, S., Sarkar, D. & Team, R.C. (2016) *_nlme: Linear and Nonlinear Mixed Effects Models_. R package version 3.1-127*. Available from: http://CRAN.R-project.org/package=nlme (accessed 30 May 2017)
Recoder, R.S. & Nogueira, C. (2007) Composição e diversidade de répteis na região sul do Parque Nacional Grande Sertão Veredas, Brasil Central. *Biota Neotropica*, 7, 267–278.
https://doi.org/10.1590/S1676-06032007000300029
Recoder, R.S., Ribeiro, M.C. & Rodrigues, M.T. (2013) Spatial variation in morphometry in *Vanzosaura rubricauda* (Squamata, Gymnophthalmidae) from open habitats of South America and its environmental correlates. *South American Journal of Herpetology*, 8, 186–197.
https://doi.org/10.2994/Sajhd1200019.1
Recoder, R.S., Werneck, F.D., Teixeira Jr., M., Colli, G.R., Sites Jr., J.W. & Rodrigues, M.T. (2014) Geographic variation and systematic review of the lizard genus *Vanzosaura* (Squamata, Gymnophthalmidae), with the description of a new species. *Zoological Journal of the Linnean Society*, 171, 206–225.
https://doi.org/10.1111/zoj.12128
Rocha, P.L.B. & Rodrigues, M.T. (2005) Electivities and resource use by an assemblage of lizards endemic to the dunes of the São Francisco River, Northeastern Brazil. *Papéis Avulsos de Zoologia*, 45, 261–284.
https://doi.org/10.1590/S0031-10492005002200001
Rodrigues, M.T. (1988) Distribution of lizards of the genus *Tropidurus* in Brazil (Sauria, Iguanidae). *In:* Vanzolini, P. & Heyer, W. (Eds.), *Proceedings of a Workshop on Neotropical Distribution Patterns*. Academia Brasileira de Ciências, Rio de Janeiro, pp. 305–315.
Rodrigues, M.T. (1991a) Herpetofauna das dunas interiores do rio São Francisco: Bahia: Brasil. 1. Introdução à área e descrição de um novo gênero de microteiideos (*Calyptommatus*) com notas sobre sua ecologia, distribuição e especiação (Sauria, Teiidae). *Papéis Avulsos de Zoologia*, 37, 285–320.
Rodrigues, M.T. (1991b) Herpetofauna das dunas interiores do rio São Francisco: Bahia: Brasil. 2. *Psilophthalmus*: um novo gênero de microteiideos sem pálpebra (Sauria: Teiidae). *Papéis Avulsos de Zoologia*, 37, 321–327.
Rodrigues, M.T. (1996) Lizards, snakes, and amphisbaenians from the quaternary sand dunes of the middle Rio São Francisco, Bahia, Brazil. *Journal of Herpetology*, 30, 513–523.

https://doi.org/10.2307/1565694
Rodrigues, M.T. (2003) Herpetofauna da Caatinga. *In:* Leal, I.R., Tabarelli, M. & Silva, J.M.C. (Eds.), *Ecologia e Conservaçao da Caatinga*. Universidade Federal de Pernambuco, Recife, pp. 181–236.
Rodrigues, M.T., Cassimiro, J., Pavan, D., Curcio, F.F., Verdade, V.K. & Pellegrino, K.C.M. (2009) A new genus of microteiid lizard from the Caparaó mountains, Southeastern Brazil, with a discussion of relationships among Gymnophthalminae (Squamata). *American Museum Novitates*, 2009, 1–27.
https://doi.org/10.1206/622.1
Rodrigues, M.T. & Juncá, F.A. (2002) Herpetofauna of the quaternary sand dunes of the middle Rio São Francisco: Bahia: Brazil. 7. *Typhlops amoipira* sp. nov., a possible relative of *Typhlops yonenagae* (Serpentes, Typhlopidae). *Papéis Avulsos de Zoologia*, 42, 325–333.
https://doi.org/10.1590/S0031-10492002001300001
Rodrigues, M.T., Pavan, D. & Curcio, F.F. (2007) Two new species of lizards of the genus *Bachia* (Squamata, Gymnophthalmidae) from Central Brazil. *Journal of Herpetology*, 41, 545–553.
https://doi.org/10.1670/06-103.1
Rodrigues, M.T. & Santos, E.M. (2008) A new genus and species of eyelid-less and limb reduced gymnophthalmid lizard from northeastern Brazil (Squamata, Gymnophthalmidae). *Zootaxa*, 1873, 50–60.
Romer, A.S. (1956) *Osteology of the Reptiles*. The University of Chicago Press, Chicago, 772 pp.
Ronquist, F. & Huelsenbeck, J.P. (2003) MrBayes 3: Bayesian phylogenetic inference under mixed models. *Bioinformatics*, 19, 1572–1574.
https://doi.org/10.1093/bioinformatics/btg180
Roscito, J.G. & Rodrigues, M.T. (2013) A comparative analysis of the post-cranial skeleton of fossorial and non-fossorial gymnophthalmid lizards. *Journal of Morphology*, 274, 845–858.
https://doi.org/10.1002/jmor.20139
Russel, A.P. & Bauer, A.M. (2008) The appendicular locomotor apparatus of Sphenodon and normal-limbed Squamates. *In:* Gans, C., Gaunt, A.S. & Adler, K. (Eds.), *Biology of the Reptilia. Vol. 21. Morphology I*. Society for the Study of Amphibians and Reptiles, Ithaca, pp. 1–465.
Savage, J.M. (1997) On terminology for the description of the hemipenes of squamate reptiles. *The Herpetological Journal*, 7, 23–25.
Stamatakis, A. (2006) RAxML-VI-HPC: maximum likelihood-based phylogenetic analyses with thousands of taxa and mixed models. *Bioinformatics*, 22, 2688–2690.
https://doi.org/10.1093/bioinformatics/btl446
Szépligeti, G. (1902) Tropische cenocoelioniden und braconiden aus der sammlung des Ungarischen National-Museums. II. *Természetrajzi Füzetek kiadja a Magyar nemzeti Muzeum*, 25, 39–84.
Tamura, K., Peterson, D., Peterson, N., Stecher, G., Nei, M. & Kumar, S. (2011) MEGA5: Molecular evolutionary genetics analysis using maximum likelihood, evolutionary distance, and maximum parsimony methods. *Molecular Biology and Evolution*, 28, 2731–2739.
https://doi.org/10.1093/molbev/msr121
Teixeira Jr., M., Prates, I., Silva-Martins, N.S., Strüssmann, C. & Rodrigues, M.T. (2015) Molecular data reveal spatial and temporal patterns of diversification and a cryptic new species of lowland *Stenocercus* Duméril & Bibron, 1837 (Squamata: Tropiduridae). *Molecular Phylogenetics and Evolution*, 94, 410–423.
https://doi.org/10.1016/j.ympev.2015.09.010
Teixeira Jr, M., Recoder, R.S., Camacho, A., Sena, M.A., Navas, C.A. & Rodrigues, M.T. (2013) A new species of *Bachia* Gray, 1845 (Squamata: Gymnophthalmidae) from the Eastern Brazilian Cerrado, and data on its ecology, physiology and behavior. *Zootaxa*, 3616 (2), 173–189.
https://doi.org/10.11646/zootaxa.3616.2.6
Thomassen, H., Gomides, S.C., Dilva, E.T., Pinto, H.B.A., Leite, F.S.F. & Garcia, P.C.A. (2016) New state record and updated geographic distribution for the little known *Psilophthalmus paeminosus* (Squamata, Gymnophthalmidae). *North-Western Journal os Zoology*, ei62504, 1–15.
Torres-Carvajal, O. & Mafla-Endara, P. (2013) A new cryptic species of *Stenocercus* (Squamata: Iguanidae) from the Andes of Ecuador. *Journal of Herpetology*, 47, 184–190.
https://doi.org/10.1670/11-211
Townsend, T.M., Alegre, R.E., Kelley, S.T., Wiens, J.J. & Reeder, T.W. (2008) Rapid development of multiple nuclear loci for phylogenetic analysis using genomic resources: An example from squamate reptiles. *Molecular Phylogenetics and Evolution*, 47, 129–142.
https://doi.org/10.1016/j.ympev.2008.01.008
Trontelj, P. & Fišer, C. (2009) Cryptic species diversity should not be trivialised. *Systematics and Biodiversity*, 7, 1–3.
https://doi.org/10.1017/S1477200008002909
Uzzell, T. (1973) A revision of lizards of the genus *Prionodactylus*, with a new genus for *P. leucostictus* and notes on the genus *Euspondylus* (Sauria, Teiidae). *Postilla*, 159, 1–67.
https://doi.org/10.5962/bhl.part.11535
Vanzolini, P.E. & Ab'Saber, A.N. (1968) Divergence rate in South American lizards of the genus *Liolaemus* (Sauria, Iguanidae).

Papéis Avulsos do Departamento de Zoologia, 21, 205–208.
Vanzolini, P.E. & Gomes, N. (1979) On *Tropidurus hygomi*: redescription, ecological notes, distribution and history (Sauria, Iguanidae). *Papéis Avulsos do Departamento de Zoologia*, 32, 243–259.
Werneck, F.P., Gamble, T., Colli, G., Rodrigues, M.T. & Sites Jr., J.W. (2012) Deep diversification and long-term persistence in the South American 'Dry Diagonal': itegrating continent-wide phylogeography and distribution modeling of geckos. *Evolution*, 66 (10), 3014–3034.
https://doi.org/10.1111/j.1558-5646.2012.01682.x
Werneck, F.P., Leite, R.N., Geurgas, S.R. & Rodrigues, M.T. (2015) Biogeographic history and cryptic diversity of saxicolous Tropiduridae lizards endemic to the semiarid Caatinga. *BMC Evolutionary Biology*, 15, 94.
https://doi.org/10.1186/s12862-015-0368-3
Zaher, H. (1999) Hemipenial morphology of the South American xenodontine snakes, with a proposal for a monophyletic Xenodontinae and a reappraisal of colubroid hemipenes. *Bulletin of the American Museum of Natural History*, 1999, 1–168.
Zar, J.H. (2014) *Biostatistical Analysis*. Pearson Education Limited, Upper Saddle River, NJ, 756 pp.

APPENDIX I. Examined material.

Collection acronyms: MNRJ = Museu Nacional, Universidade Federal do Rio de Janeiro; MZUSP = Museu de Zoologia da Universidade de São Paulo; AAG = Adrian Garda, field number; RPD = Roberta Pacheco Damasceno, field number; ACG = Agustín Camacho Guerrero, field number; MZUESC = Museu de Zoologia da Universidade Estadual de Santa Cruz; FSFL = Felipe Sá Fortes Leite, field number; MTR = Miguel Trefaut Rodrigues, field number; MUFAL = Museu da Universidade Federal de Alagoas.

Psilops seductus **(n=12): BRAZIL: Bahia:** Jaborandi: MNRJ 1097–19105, MNRJ 19117, MNRJ 19118 (stained); **Minas Gerais:** Formoso: MZUSP 94703.

Psilops mucugensis **(n=31): BRAZIL: Bahia:** Palmeiras: AAG 6640, AAG 6652, AAG 6663, AAG 6692, AAG 6715–6716, AAG 7026, AAG 7040–7041, AAG 7065, AAG 7080, AAG 7109, AAG 7120, AAG 7142, AAG 7144, AAG 7190, AAG 7199, AAG 7220, AAG 7228, AAG 7249, AAG s/n (2 ex.); Mucugê: MZUSP 96918 (stained), MZUSP 106187–106188; Miguel Calmon: MZUSP 106194, MZUSP 106196, MZUSP 106208–106210; Morro do Chapéu: MZUSP 106206.

Psilops paeminosus **(n=70): BRAZIL: Bahia:** Gentio do Ouro, Gameleira do Assuruá: MZUSP 106186; Lagoa de Itaparica: MZUSP 77982–77985; Nova Barra do Tarrachil: MZUSP 74232; Novo Triunfo, Casa das Fortunas: MZUSP 106207; Raso da Catarina: MZUSP 106211–106214, MZUSP 106218; Santa Brígida, Morada Velha: MZUSP 106200, MZUSP 106199, MZUSP 106201; Santo Inácio: MZUSP 74232, MZUSP 74959, MZUSP 76226–76230, MZUSP 76234–76235, MZUSP 76239, MZUSP 76410, MZUSP 79753–79757, MZUSP 103258, MZUSP 106186, MZUSP 106217; Vitoria da Conquista: MZUSP 71904, MZUSP 74227–74228, MZUESC 3732, MZUESC 3735, MZUESC 3737–3738, MZUESC 3741, MZUESC 3755–3756, MZUSP 106202–106205. **Minas Gerais:** Grão Mogol: MZUSP 106189–106195; Serranópolis de Minas: FSFL 1183, FSFL 1184. **Sergipe:** Canindé do São Francisco: MUFAL 6271–6278, MUFAL 6280–6281, MUFAL 6285, MZUSP 106198.